JÜLICH
FORSCHUNGSZENTRUM

Membrane biophysics investigated by multiscale methods

September 24, 2013

Paolo Carloni

Institute for Computational Medicine (IAS-5) and German Research School,

Juelich Research Center and RWTH-Aachen

Cell Membrane

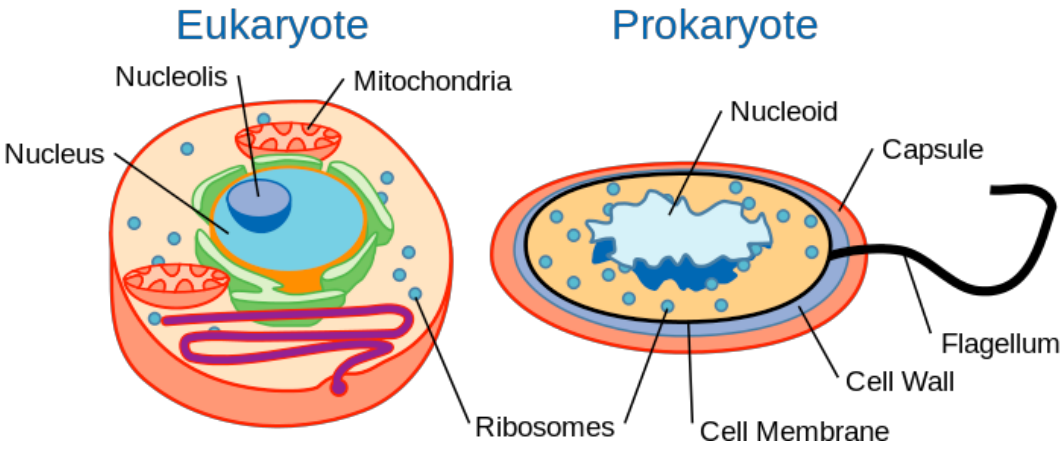

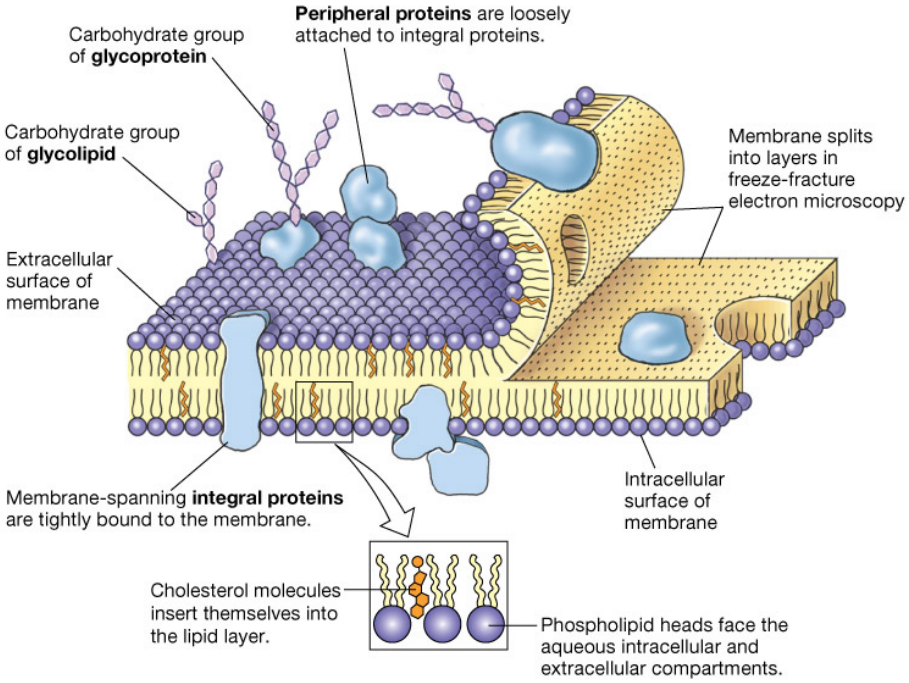

Ions and chemicals across and thru membranes

Proton Transfer

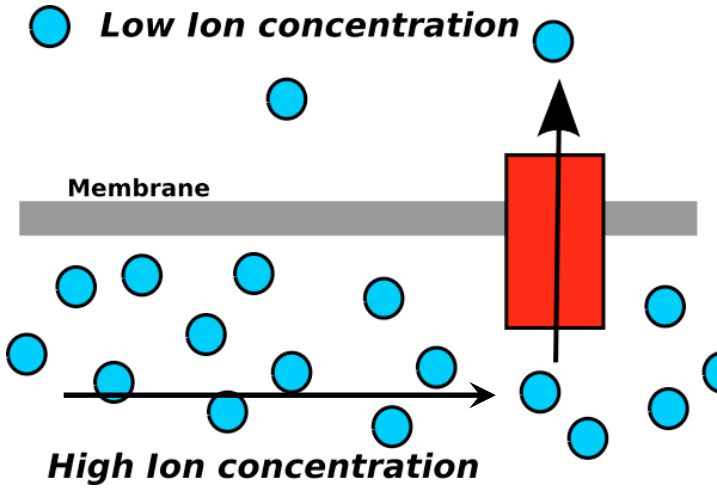

Metal Ion Transfer

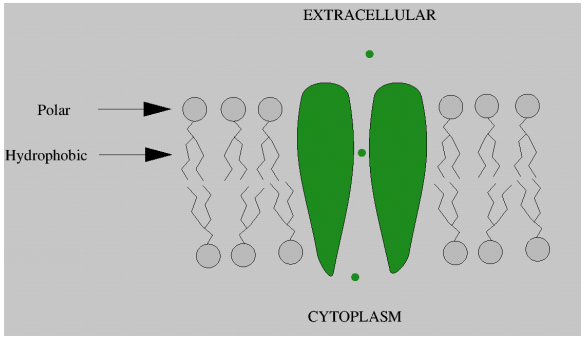

Binding of chemicals

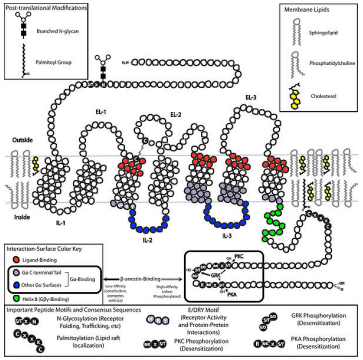

Lateral proton transfer: a minimalistic model

- Peter Pohl (University of Linz): escape free energy: 8.7 RT and D =5.7 10^{-5} cm^2s^{-1} for water/n-decane

- At water/vapor interface, *ab-initio MD* and MS-EVB simulations revealed the acidification of the top surface water layer as compared to bulk water

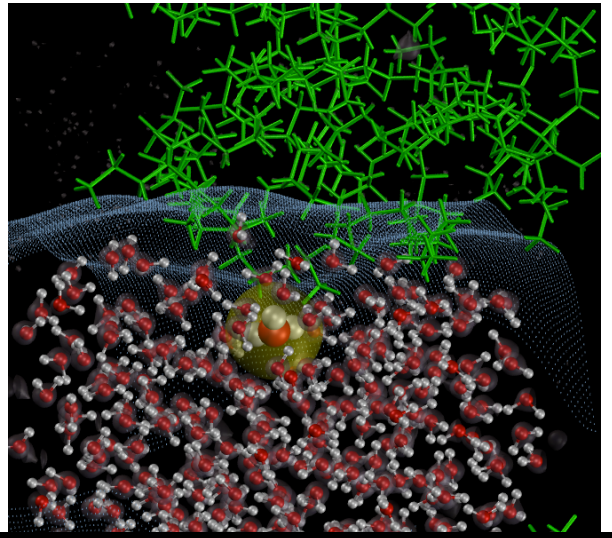

Petersen et al (2004) J Phys Chem B 108:14804-14806.
Buch et al. Proc Natl Acad Sci USA 104: 7342-7347.
Köfinger & Dellago C (2008) J Phys Chem B 112: 2349-2356.
Lee & Tuckerman (2009) J Phys Chem A 113: 2144-2151.

- Free energy minima about 3 Å wide from the interface found in MS-EVB simulations at water/ carbon nanotubes and water/CCl_4 interfaces

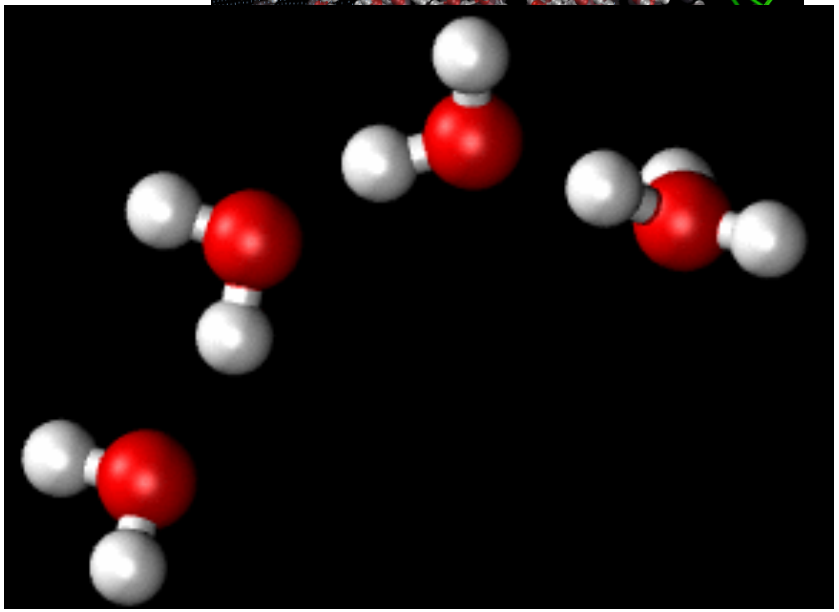

Dellago & Hummer G (2006). Phys Rev Lett 97:245901.
Luchi et al. (2009) J Phys Chem B 113:4017-4030.

Ab initio MD simulations of Proton Transfer

JUGENE, a 72-rack IBM BlueGene/P supercomputer at JSC

≈ 295.000 cores

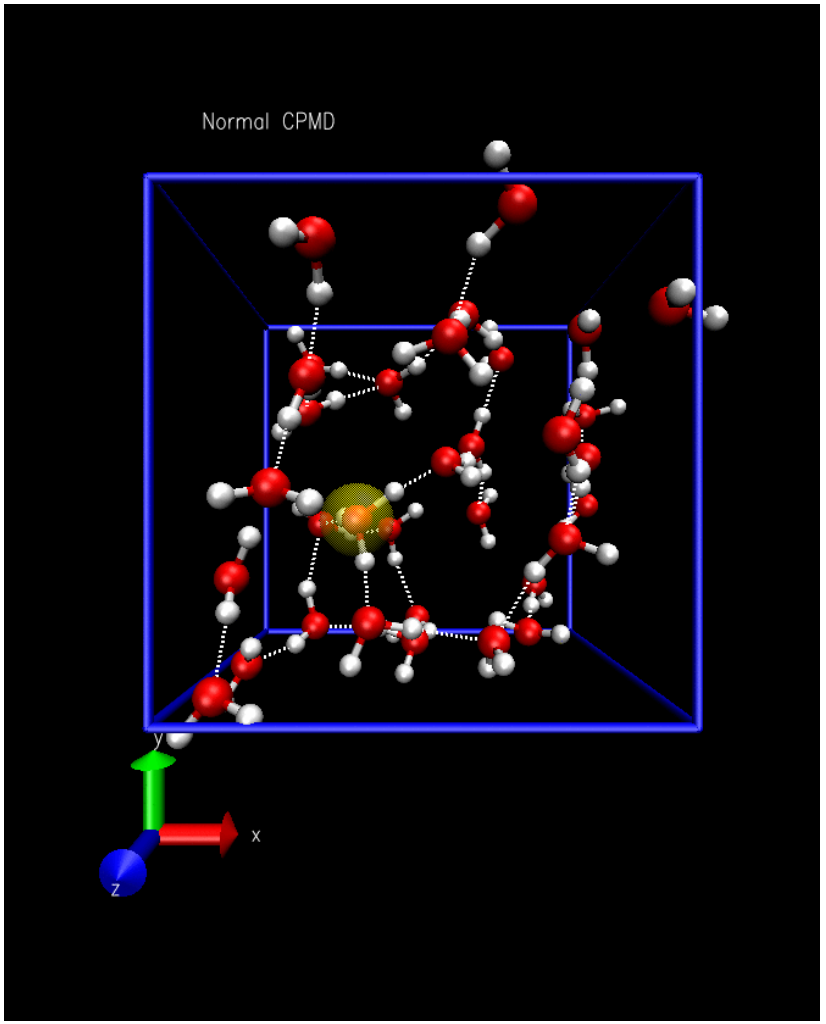

Marx D, Tuckerman ME, Hutter J, Parrinello M (1999). Nature 397:601–604.
Park, Laio, Iannuzzi and Parrinello, J. Am. Chem. Soc., 2006, 128: 11318

Car-Parrinello molecular dynamics

$$L_{CPMD} = \frac{1}{2}\sum_I M_I \dot{\mathbf{R}}_I^2 + \frac{1}{2}\mu\sum_i \int d\mathbf{r} \left|\dot{\varphi}_i(\mathbf{r})\right|^2 - V_{DFT}(\mathbf{R},\mathbf{r}) + \sum_i\sum_j \Lambda_{ij}\left(\int d\mathbf{r}\varphi_i^*(\mathbf{r})\varphi_j(\mathbf{r}) - \delta_{ij}\right)$$

$$V_{DFT}(\mathbf{R},\mathbf{r}) = \sum_I\sum_{I<J}\frac{Z_I Z_J}{|\mathbf{R}_I - \mathbf{R}_J|} - \frac{1}{2}\sum_i \int d\mathbf{r}\varphi_i^*(\mathbf{r})\nabla^2\varphi_i(\mathbf{r}) + \frac{1}{2}\int d\mathbf{r}\, d\mathbf{r}' \frac{\rho(\mathbf{r})\rho(\mathbf{r}')}{|\mathbf{r}-\mathbf{r}'|} + E_{XC}[\rho(\mathbf{r})] + \int d\mathbf{r} V_{Ne}\rho(\mathbf{r})$$

$$\rho(\mathbf{r}) = \sum_i |\varphi_i(\mathbf{r})|^2$$

μ = fictitious mass Λ_{ij} = Lagrange multiplier

Car and Parrinello, Phys. Rev. Lett. 1985, 55: 2471

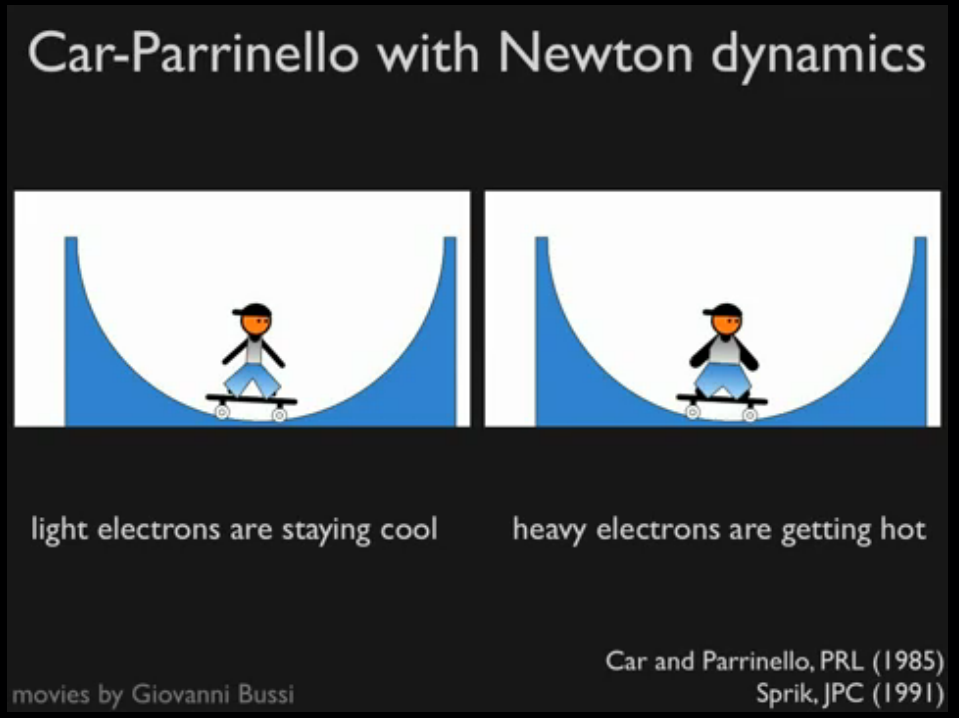

CPMD on a very large system

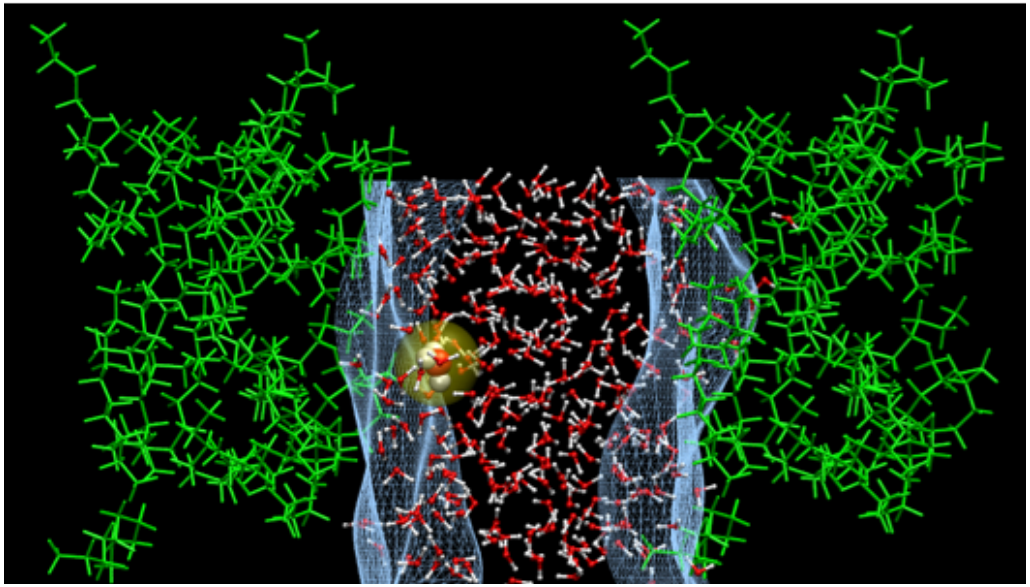

System:

- 25 decane molecules
- 303 H_2O
- 1 H^+

  = 1707 atoms

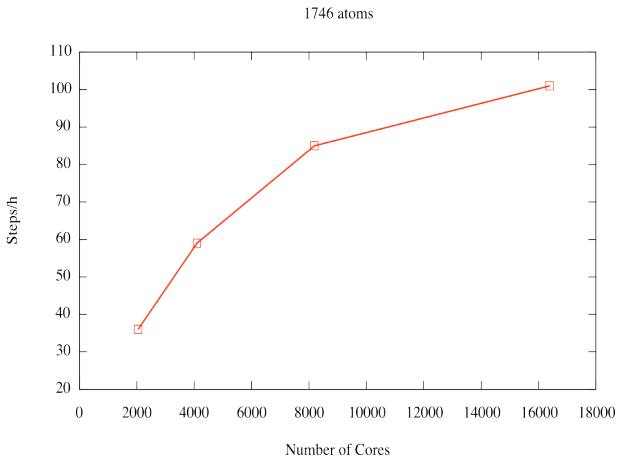

A. Curioni, IBM Zurich Research Lab

- CPMD - DFT/BLYP
- Plane-waves
- Pseudopotentials
- www.cpmd.org

CPMD on a very large system

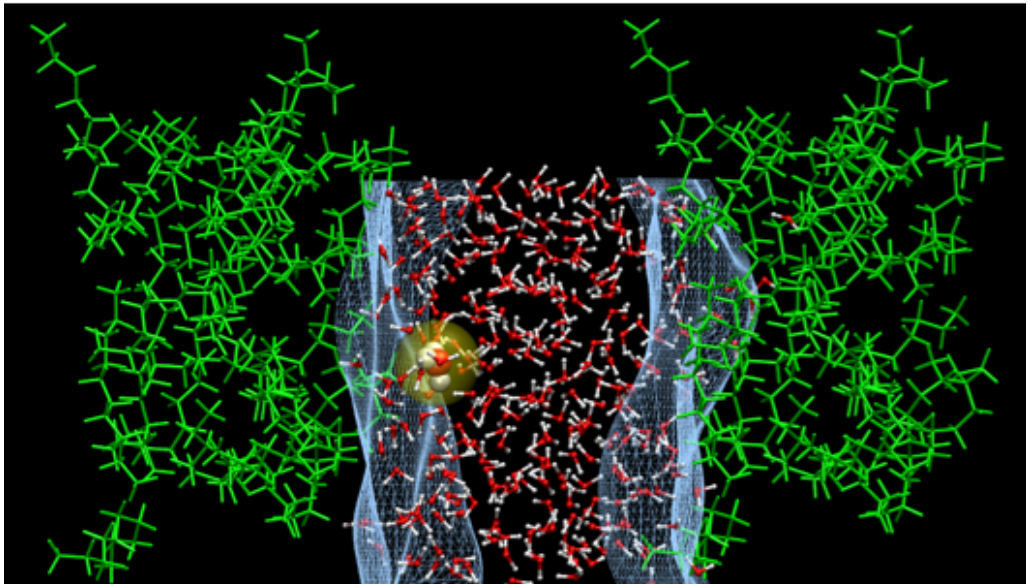

System:

- 25 decane molecules
- 303 H_2O
- 1 H^+

  = 1707 atoms

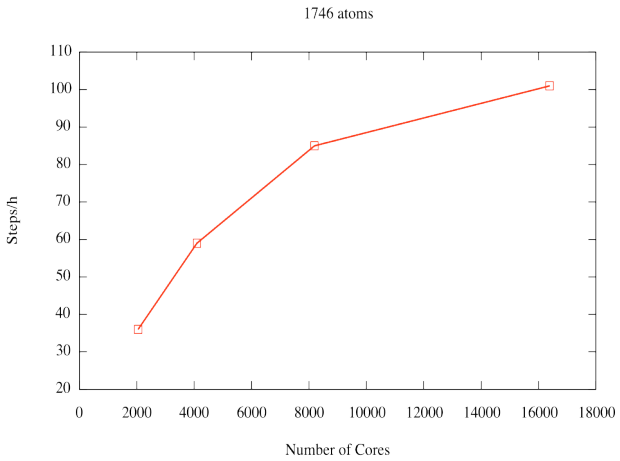

A. Curioni, IBM Zurich Research Lab

- CPMD - DFT/BLYP
- Plane-waves
- Pseudopotentials
- www.cpmd.org

- Empirical dispersion correction (Grimme *J. Comp. Chem.* **2006**, 27, 1787.)

Balancing computer efficiency and accuracy

Grimme's correction for the dispersion forces

Grimme (2004) J Comput Chem 25:1463-1473.

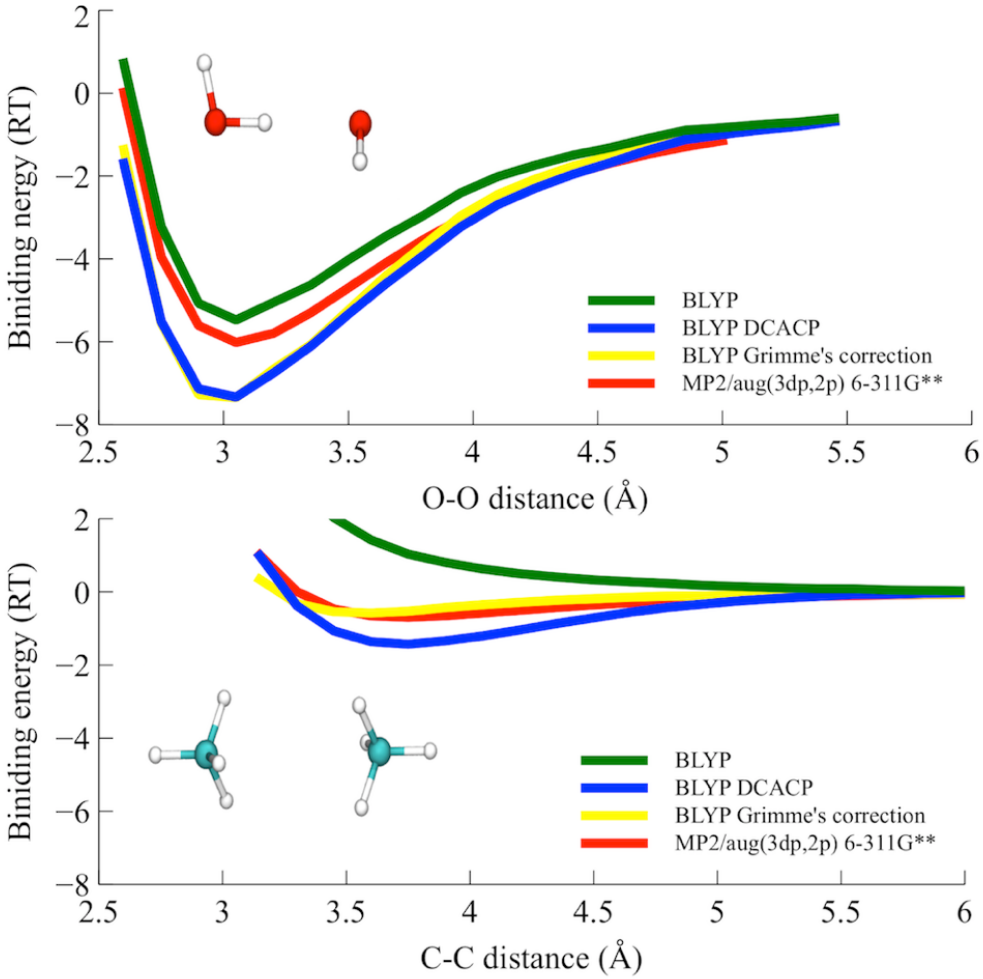

Car-Parrinello molecular dynamics

$$L_{CPMD} = \frac{1}{2}\sum_I M_I \dot{\mathbf{R}}_I^2 + \frac{1}{2}\mu\sum_i \int d\mathbf{r} \left|\dot{\varphi}_i(\mathbf{r})\right|^2 - V_{DFT}(\mathbf{R},\mathbf{r}) + \sum_i\sum_j \Lambda_{ij}\left(\int d\mathbf{r}\varphi_i^*(\mathbf{r})\varphi_j(\mathbf{r}) - \delta_{ij}\right)$$

$$V_{DFT}(\mathbf{R},\mathbf{r}) = \sum_I\sum_{I<J}\frac{Z_I Z_J}{|\mathbf{R}_I - \mathbf{R}_J|} - \frac{1}{2}\sum_i \int d\mathbf{r}\varphi_i^*(\mathbf{r})\nabla^2\varphi_i(\mathbf{r}) + \frac{1}{2}\int d\mathbf{r}\, d\mathbf{r}' \frac{\rho(\mathbf{r})\rho(\mathbf{r}')}{|\mathbf{r}-\mathbf{r}'|} + E_{XC}[\rho(\mathbf{r})] + \int d\mathbf{r} V_{Ne}\rho(\mathbf{r})$$

$$\rho(\mathbf{r}) = \sum_i |\varphi_i(\mathbf{r})|^2$$

μ = fictitious mass Λ_{ij} = Lagrange multiplier

Car and Parrinello, Phys. Rev. Lett. 1985, 55: 2471

Dynamics

$$D = \lim_{t\to\infty}\frac{1}{6t}\sum_I \left\langle \left|\mathbf{R}_I(t) - \mathbf{R}_I(0)\right|^2 \right\rangle$$

Energetics

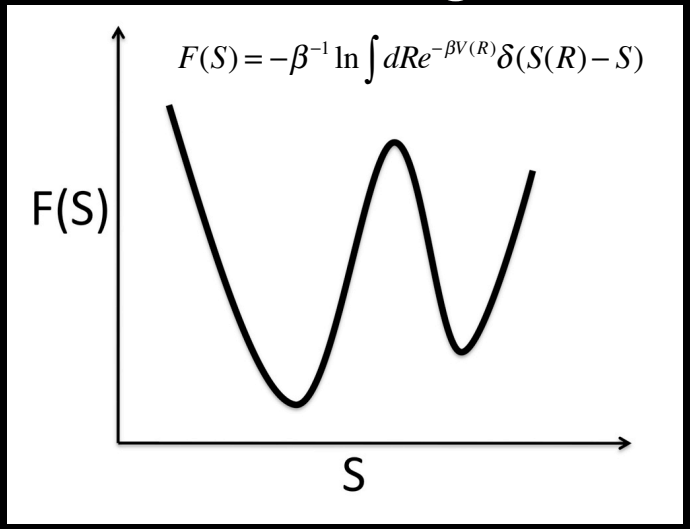

S = collective variable

Enhanced sampling method: Metadynamics

$$V_{bias}(s,t) = \sum_{t'=\tau,2\tau,\cdots<t} w \exp(-\frac{(s-s(t))^2}{2\sigma^2})$$

w = hill width

σ = hill height

$$F(S) \simeq -\lim_{t\to\infty} V_{bias}(s,t) + C$$

Laio and Parrinello (2002), *Proc. Natl. Acad. Sci USA*, 99: 12562

Leone et al. Curr. Op. Struct. Biol. 2010

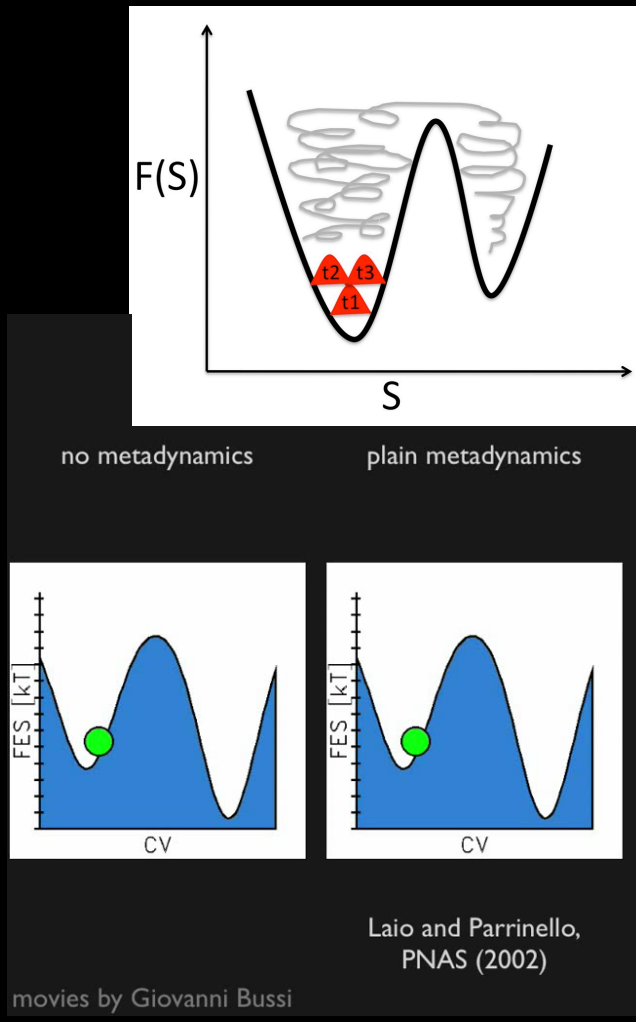

CPMD-Metadynamics on a very large system

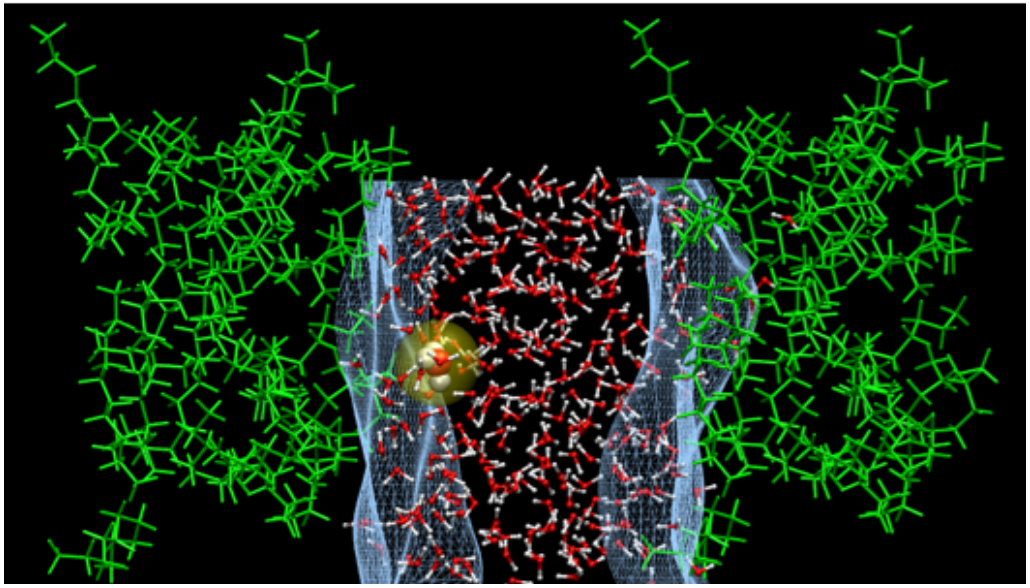

System:

- 25 decane molecules
- 303 H_2O
- 1 H^+

  = 1707 atoms

PRACE

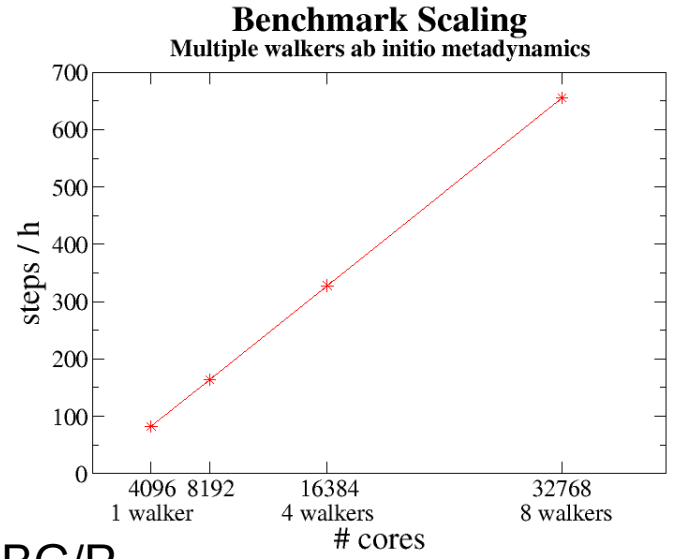

40.5 million core hours on BG/P

Collective variable *S*

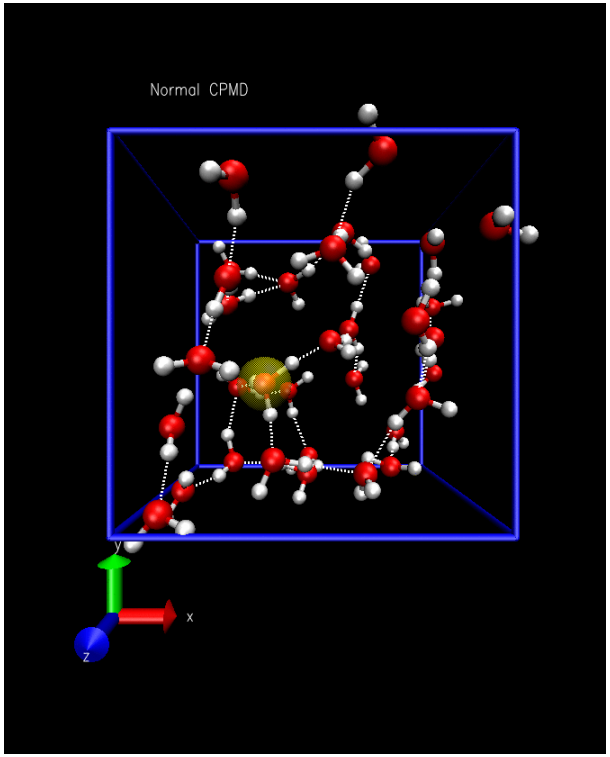

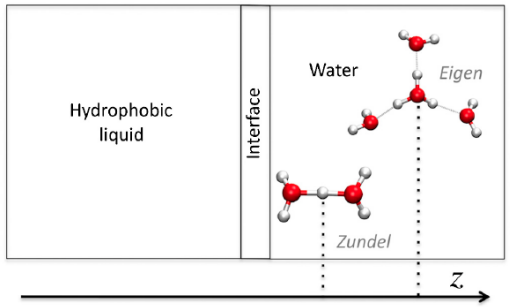

coordination number for oxygen atoms

$$n_i = \sum_{j \in \{H_w\}} n(r_{ij})$$

$$n(r_{ij}) = \frac{1 - \left(\frac{r_{ij} - d_0}{r_0} \right)^6}{1 - \left(\frac{r_{ij} - d_0}{r_0} \right)^{12}}$$

$$S = \frac{\sum_{i \in \{O_w\}} z_i \, e^{\lambda n_i}}{\sum_{i \in \{O_w\}} e^{\lambda n_i}}$$

Average of oxygen atom "weighted" positions = position of the excess proton

Park, Laio, Iannuzzi and Parrinello, J. Am. Chem. Soc., 2006, 128: 11318

Zhang, Knyazev, Vereshchaga, Ippoliti, Nguyen, Carloni and Pohl. Proc. Natl. Acad. Sci USA, 2012, 109: 9744.

Free energy as a function of *S*

Free energy profile

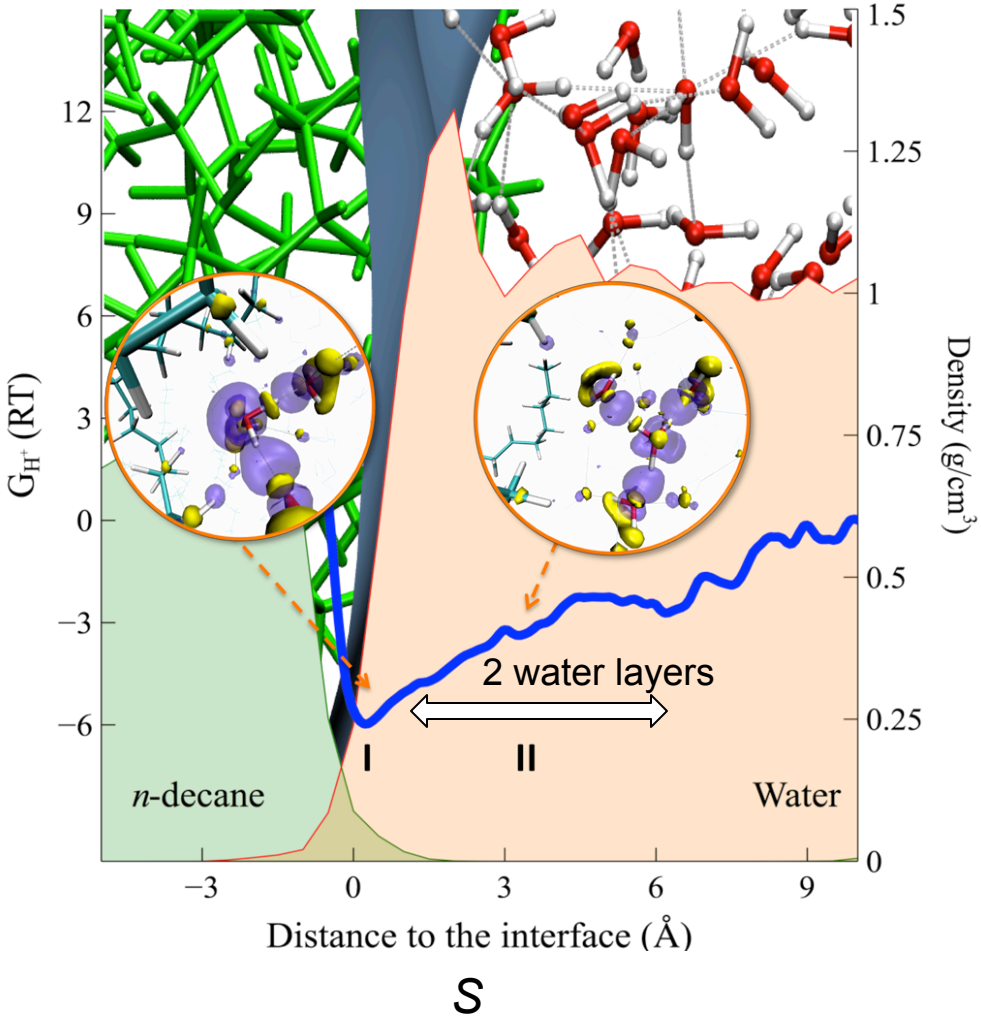

S

75 ps-long CPMD-based on metadynamics at 310 K.
G function of the distance from the excess proton to the water/*n*-decane instantaneous interface.

Wide minimum within 6 Å from the hydrophobic surface with a depth of about 6 *RT*

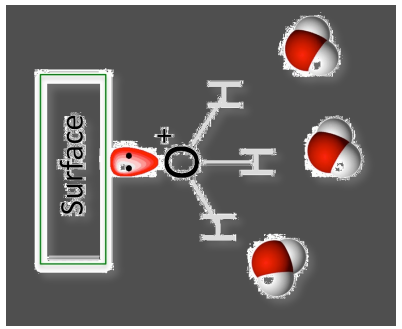

Kudin, Car *J. Am.. Chem. Soc.* **2008**, *130*, 3915.

Free energy as a function of *S*

Free energy profile

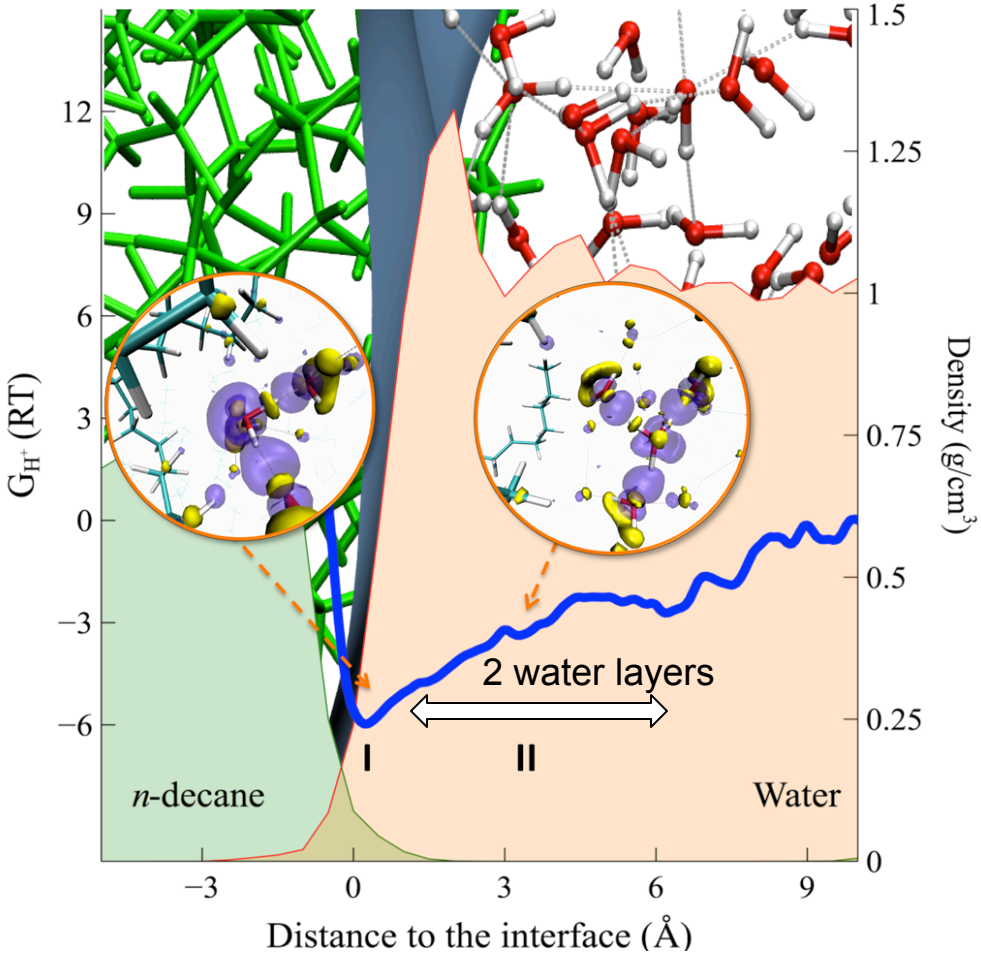

S

Free energy barrier

	$\Delta G^{\ddagger}_{H+}$
CPMD	6+/-2 *RT*
Exp.	8.7 *RT*

-Presence of a minimum consistent with P. Pohl's experiments and with EVB

-Minimum wider than that of EVB

Luchi et al. *J. Phys. Chem. B* **2009**, *113*, 4017.

Park, Laio, Iannuzzi and Parrinello, J. Am. Chem. Soc., 2006, 128: 11318

Excess proton at water/decane interface

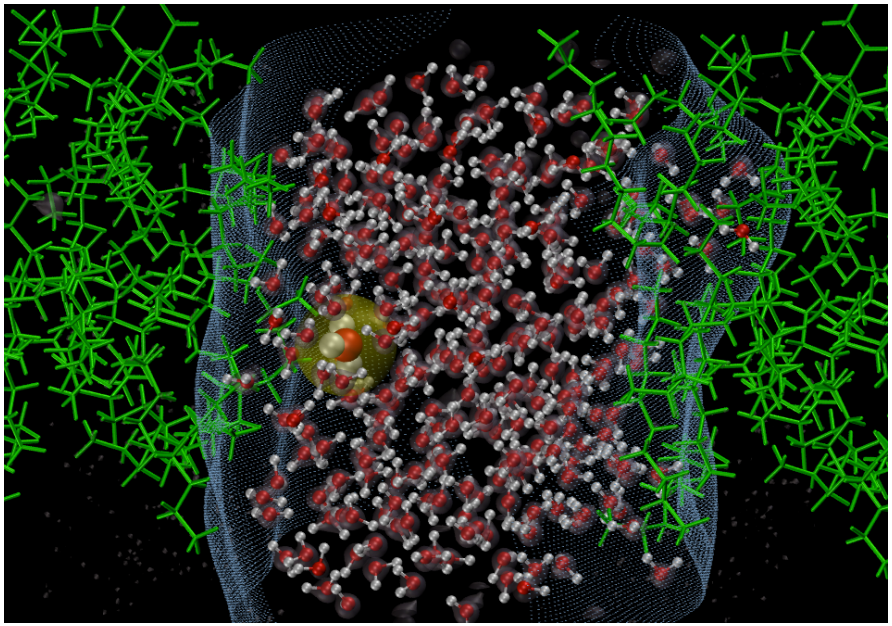

Diffusion coefficient

Method	$D \times 10^{-5} cm^2 s^{-1}$
CPMD	8±2
Exp.	5.7±0.7

- Fast diffusion of 2nd layer of interfacial water molecules

Limitations and conclusions

1. Model contains neither ions nor buffer molecules. However, varying the concentration of both kinds of molecules in the experimental system did not altered significantly the measured quantities
2. XC functional
3. Convergence issues/ collective variables
4. System size

Fast diffusion is an intrinsic properties of hydrophobic liquid/water interfaces, ***where proton may be present in more than one layer***

Diffusive proton at the second interfacial water layer

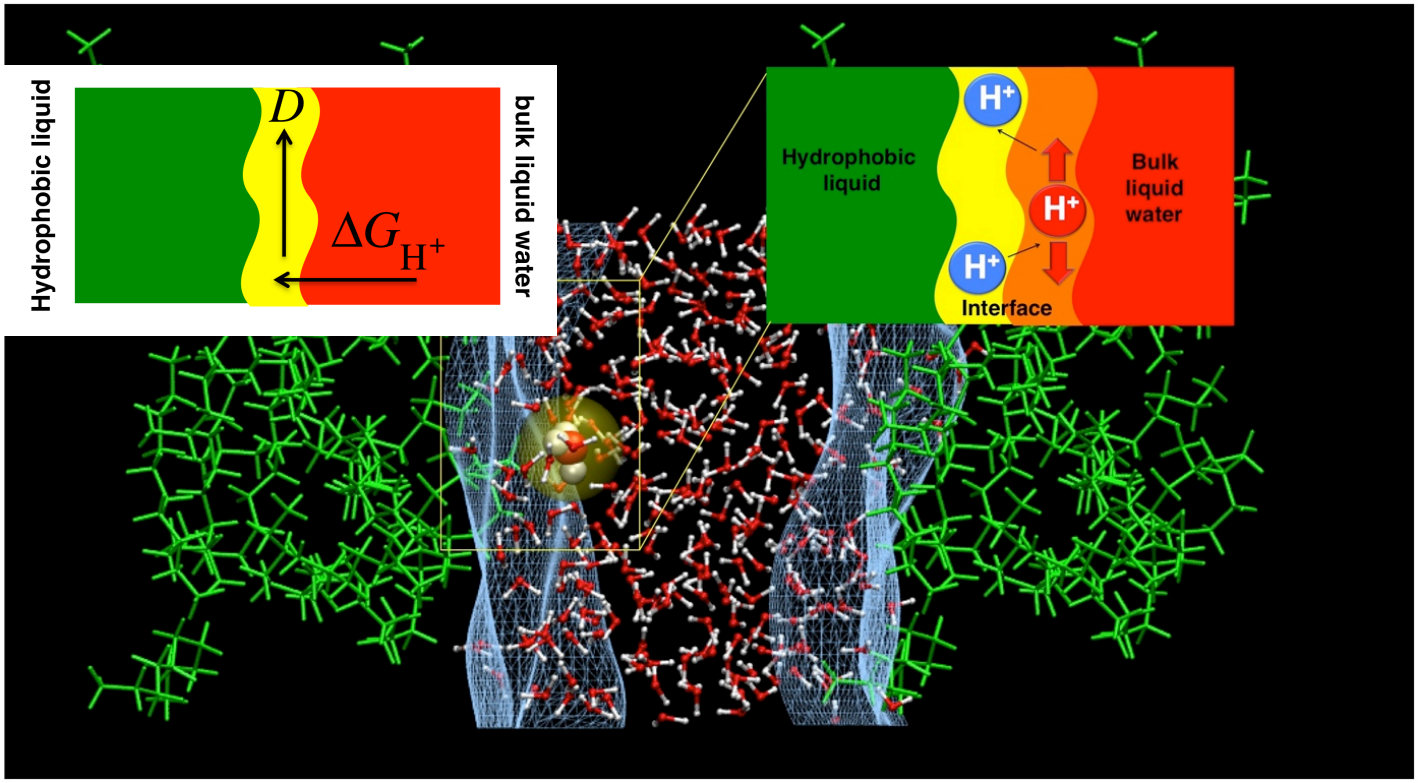

Protons located at the second interfacial water layer from the surface migrate very quickly and yet experience sufficient attractive forces to prevent release to the bulk water

Zhang, Knyazev, Vereshchaga, Ippoliti, Nguyen, PC, Pohl, *Proc. Nat. Acad. Sci., 2012*

In progress

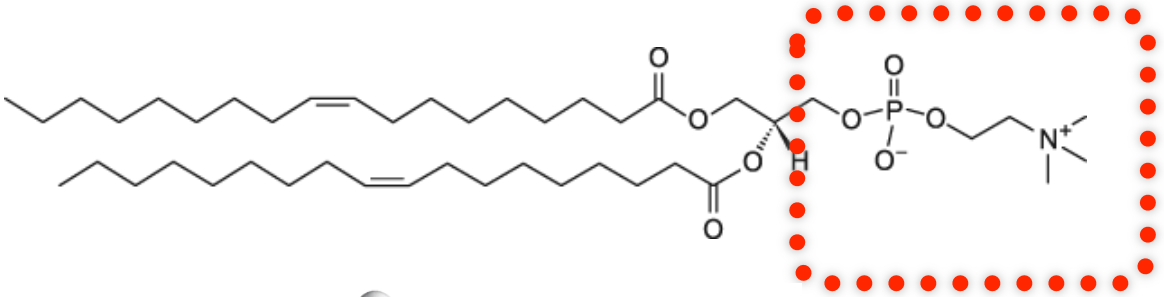

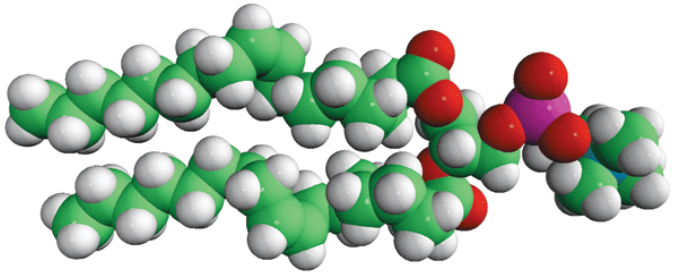

H^+ ?

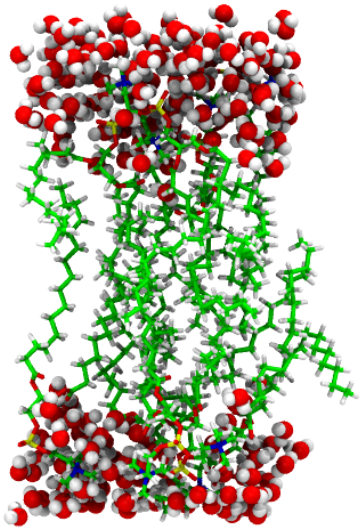

- EVB Escape free energy 6.7-8.3 RT Yamashita T, Voth GA (2010). J Phys Chem B 114: 592-603.

- D = 4-6 $\times 10^{-5}$ cm^2 s^{-1} for membrane Springer et al. Proc. Natl. Acad. Sci USA, 2011, 108, 14461.

http://www.prace-ri.eu/PRACE-5thRegular-Call

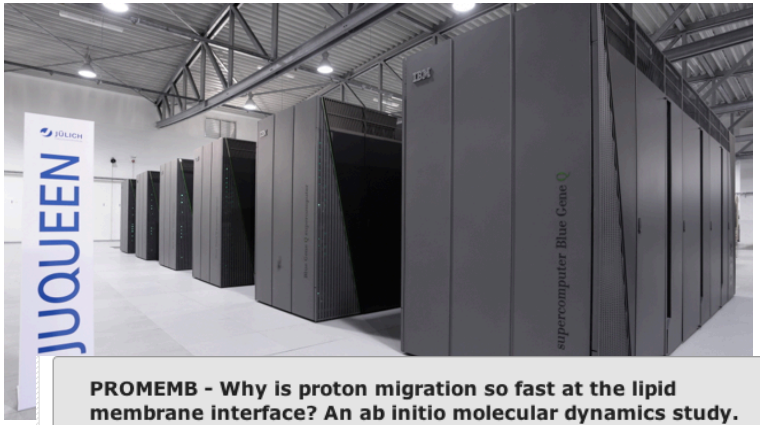

PROMEMB - Why is proton migration so fast at the lipid membrane interface? An ab initio molecular dynamics study.

Ions and chemicals across And thru membranes

Proton Transfer

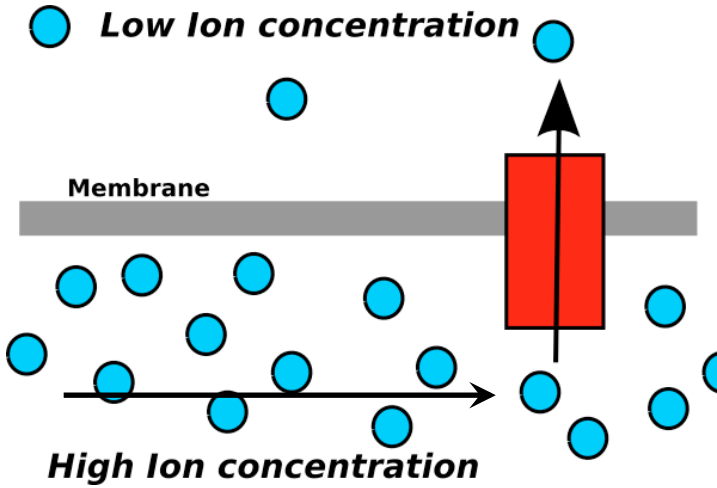

Metal Ion Transfer

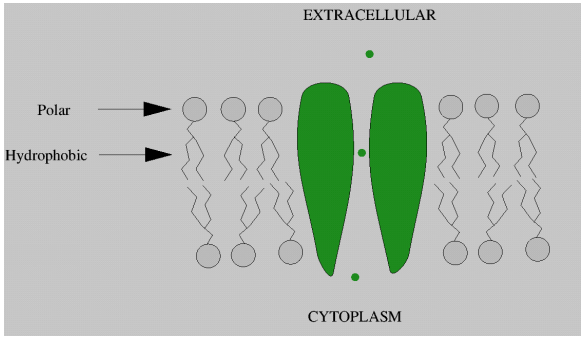

Binding of chemicals

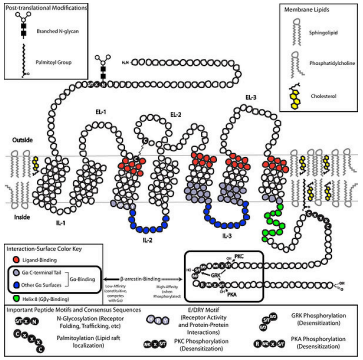

Proton@Gramicidin A

Peptide from soil bacterium *Bacillus Brevis*;

Antibiotic against gram-positive bacteria;

Fastest H^+ channel, the rate is up to $2x10^9$ H^+ s^{-1}.

Two pentadecapeptides with alternating D- and L-amino acids forming beta-helix;

Pore radius of about 3 Å

Peptide carbonyl groups pointing inwards.

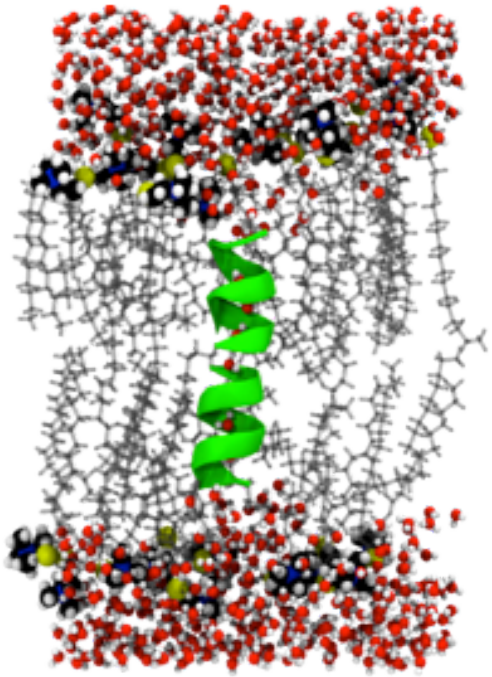

What is the physical basis for fast proton permeation ?

Physical basis of fast proton permeation by empirical calculations

JÜLICH FORSCHUNGSZENTRUM

1. Water chain reorganization [1]
2. Desolvation electrostatic energy [2]
3. Local ordering of interfacial water molecules at the membrane [3].

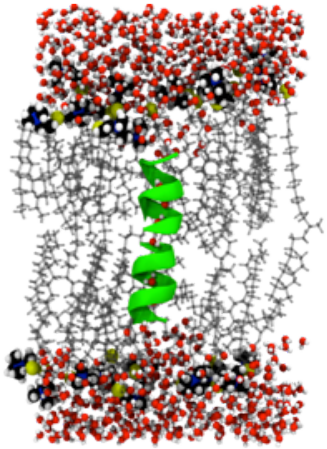

[1] Roux, *Acc. Chem. Res.* 2002, 35: 366.
[2] Braun-Sand, Burykin, Chu and Warshel, *J. Phys. Chem. B* 2005, 109: 583.
[3] Qin, Tepper and Voth, *J. Phys. Chem. B* 2007, 111: 9931.

The dipole potential

Alignment of the dipolar residues of the lipids and the partial alignment of water molecules at the membrane/solvent interface. It reflects the electrostatic potential difference at the dielectric mismatched membrane and water regions.

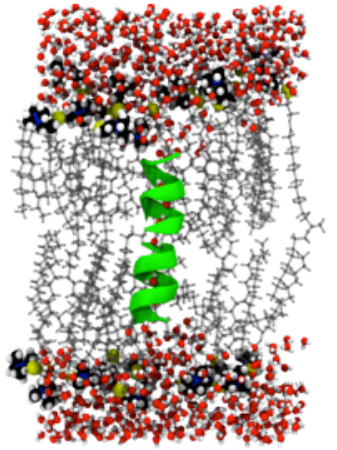

Wang, L. *Ann. Rev. Biochem.* **2012**, *81*, 615. .

The dipole potential

Experimentally

Membrane	$[H^+]_{bulk}$ [M]	G_{H^+} [pS]	ΔV_{DP} [V]
GMO	0.1	~190	0.100 ± 0.009
	1.0	~1000	0.100 ± 0.009
DPhPC	0.1	~200	0.228 ± 0.005
	1.0	789±12	0.228 ± 0.005
DPPC	1.0	664±38	0.243 ± 0.004
DOPC	1.0	660±9	0.275

Wang, L. *Ann. Rev. Biochem.* **2012**, *81*, 615

Theoretically:

Induced polarization effects – lacking in semi-empirical approaches – have been suggested to be an indispensable ingredient of dipole potentials

Harder, E.; MacKerell, A. D.; Roux, B. *J. Am. Chem. Soc.* **2009**, *131*, 2760.

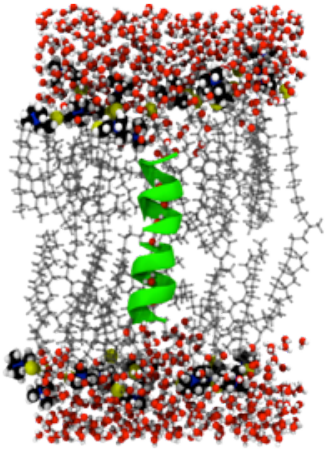

Computational Setup

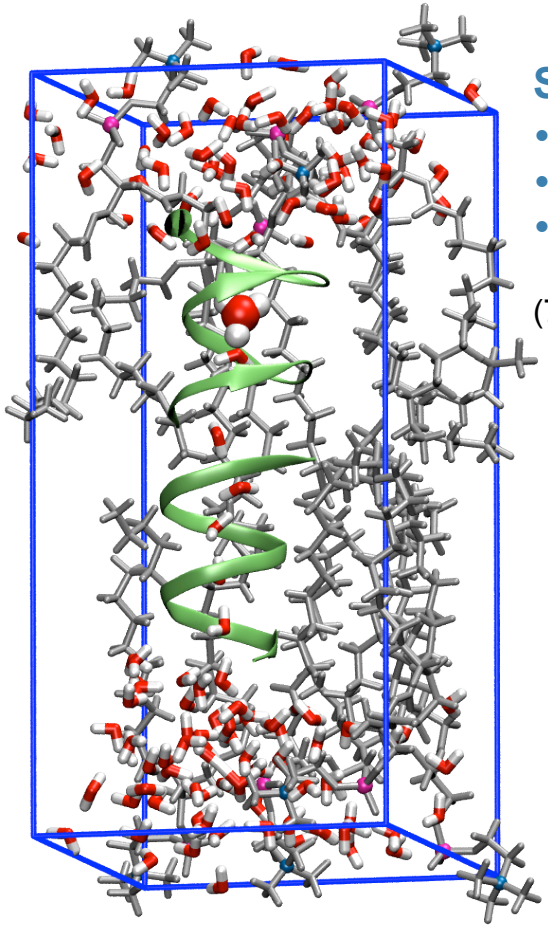

System

- Gramicidin A dimer: 552 atoms
- Lipid bilayer: 8 DMPC molecules (exp. ratio): 944 atoms
- 138 water molecules: 414 atoms

= 1911 atoms total

(7-9 water molecules inside the channel)

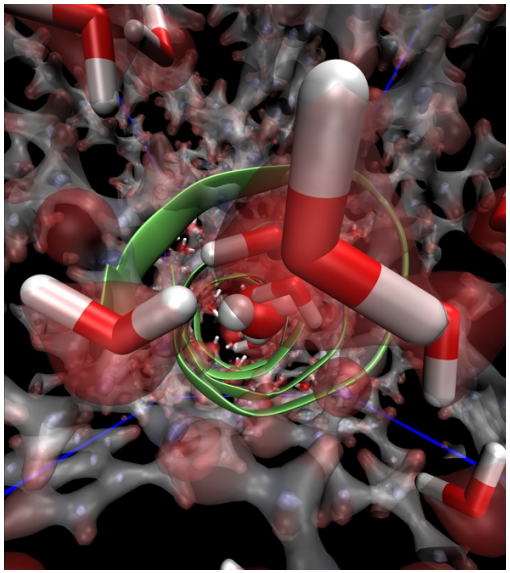

Electronic density

Method

- Density functional theory (BLYP)
- Plane-wave basis set
- Pseudopotentials
- Empirical dispersion corrections

(Grimme *J. Comp. Chem.* **2006**, 27, 1787.)

http://www.prace-project.eu/

Results: The dipole Potential

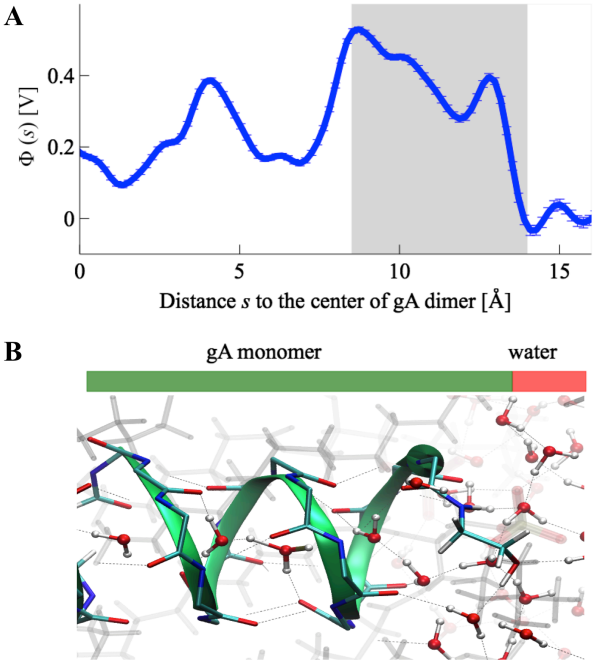

$$\Phi(s) = \frac{1}{A}\int\int\int d^3\mathbf{r}\left\langle \Phi(\mathbf{r})\delta\left(d(\mathbf{r}) - s\right)\right\rangle$$

1. Calculated free energy barrier is located at the channel entrance. Consistent with experiment

2. Membrane dipole potential (~0.4 V) rises at the channel mouth. Consistent with the experimentally observed increase of the proton permeation rate in the presence of a transmembrane voltage

Decoursey, *Physiolog. Rev*. 83, 475 (2003)

Results: Water molecules' electronic structure

1. Point charge model in commonly used force fields cannot capture the intricate changes of waters' electronic structure to a varying highly polar environment
2. Aqueous-like environment
   Indeed, the water averaged dipole moments are similar to those of pure bulk water, as measured by X-ray and neutron scattering experiments (2.9 ± 0.6 D) and ab initio MD water

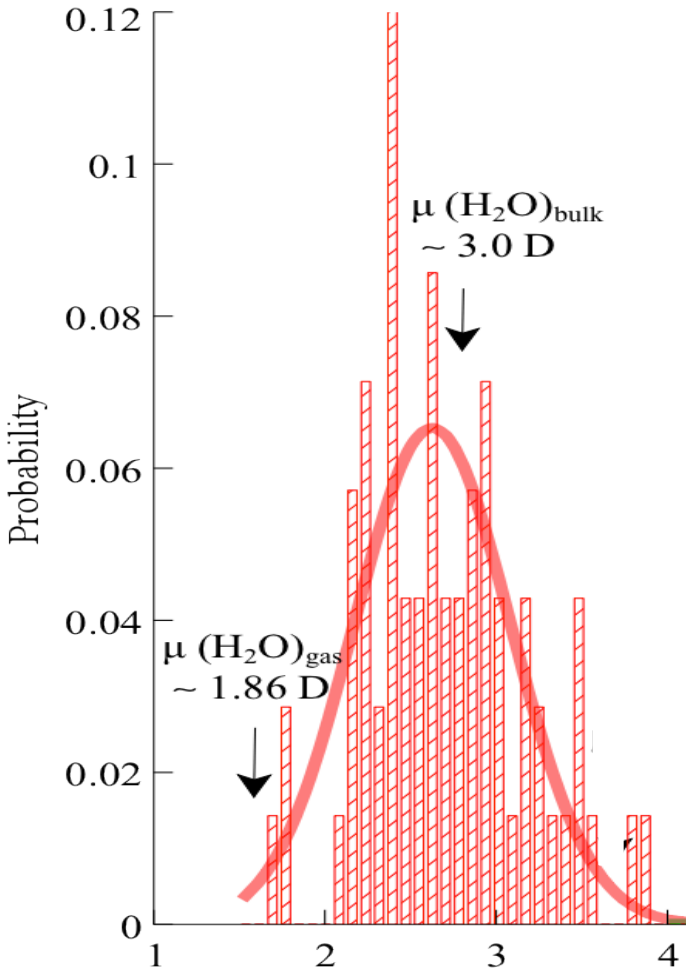

Silvestrelli, P. L.; Parrinello, M. *Phys. Rev. Lett.* **1999**, *82*, 3308.

Conclusions and Limitations

Findings consistent with the available experimental data
the membrane dipole potential plays a role for the free energy barrier at the channel mouth. This provides an explanation for the fact that the rate of proton conduction increases dramatically in the presence of a transmembrane potential.

Size of the system
BLYP calculations
nuclear quantum effects
sampling issues.

Ions and chemicals across And thru membranes

Proton Transfer

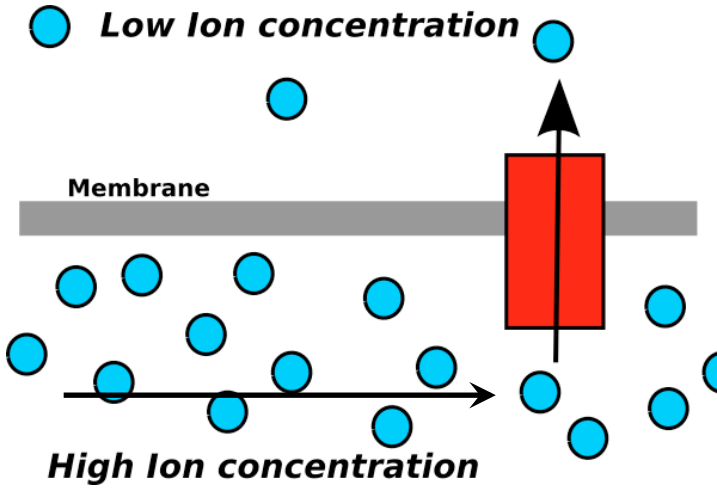

Metal Ion Transfer

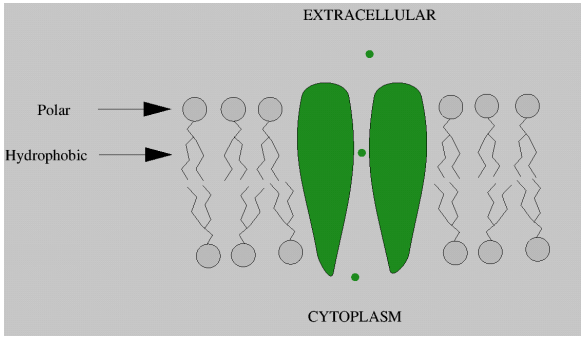

Binding of chemicals

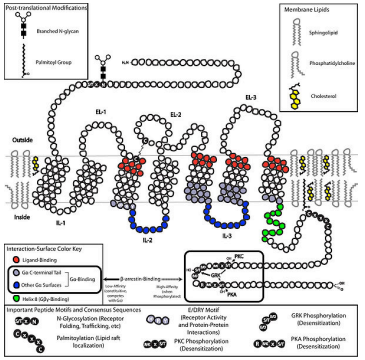

The KcsA K^+ channel

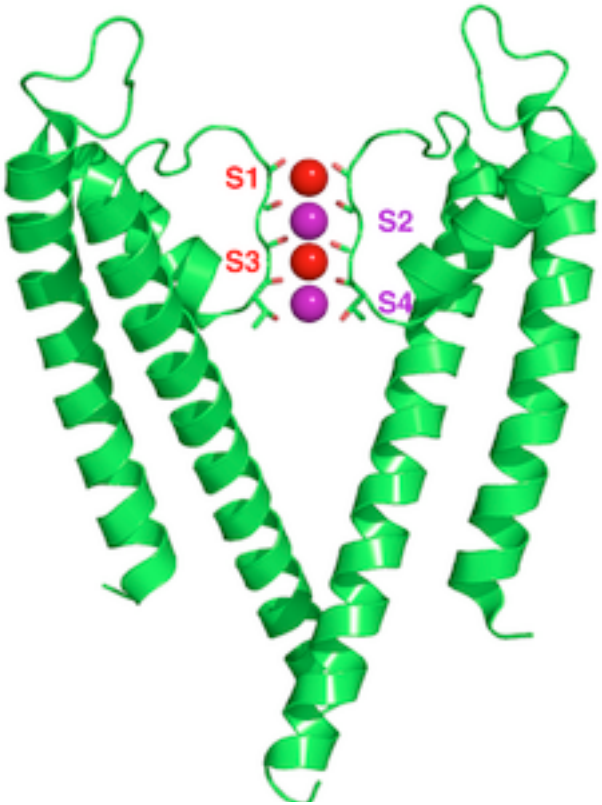

$$\mathcal{L} = \frac{1}{2}\mu \sum_i \int \mathrm{d}\mathbf{r}\, \dot{\phi}_i^*(\mathbf{r})\dot{\phi}_i(\mathbf{r}) + \frac{1}{2}\sum_I M_I \dot{\mathbf{R}}_I^2 + \frac{1}{2}\sum_{I'} M_I \dot{\mathbf{R}}_{I'}^2 - E_{MM} - E_{QM/MM} - E_{QM} +$$

$$+ \sum_{i,j} \Lambda_{i,j} \left(\int \mathrm{d}\mathbf{r}\, \phi_i^*(\mathbf{r})\phi_j(\mathbf{r}) - \delta_{i,j} \right)$$

$$E_{QM} = E_{KS}[\phi_i, \mathbf{R}_I]$$

Roethlisberger et al. 2002
Dal Peraro et al. Curr Op. Str.Biol 2007

The all-atom potential E_{MM}

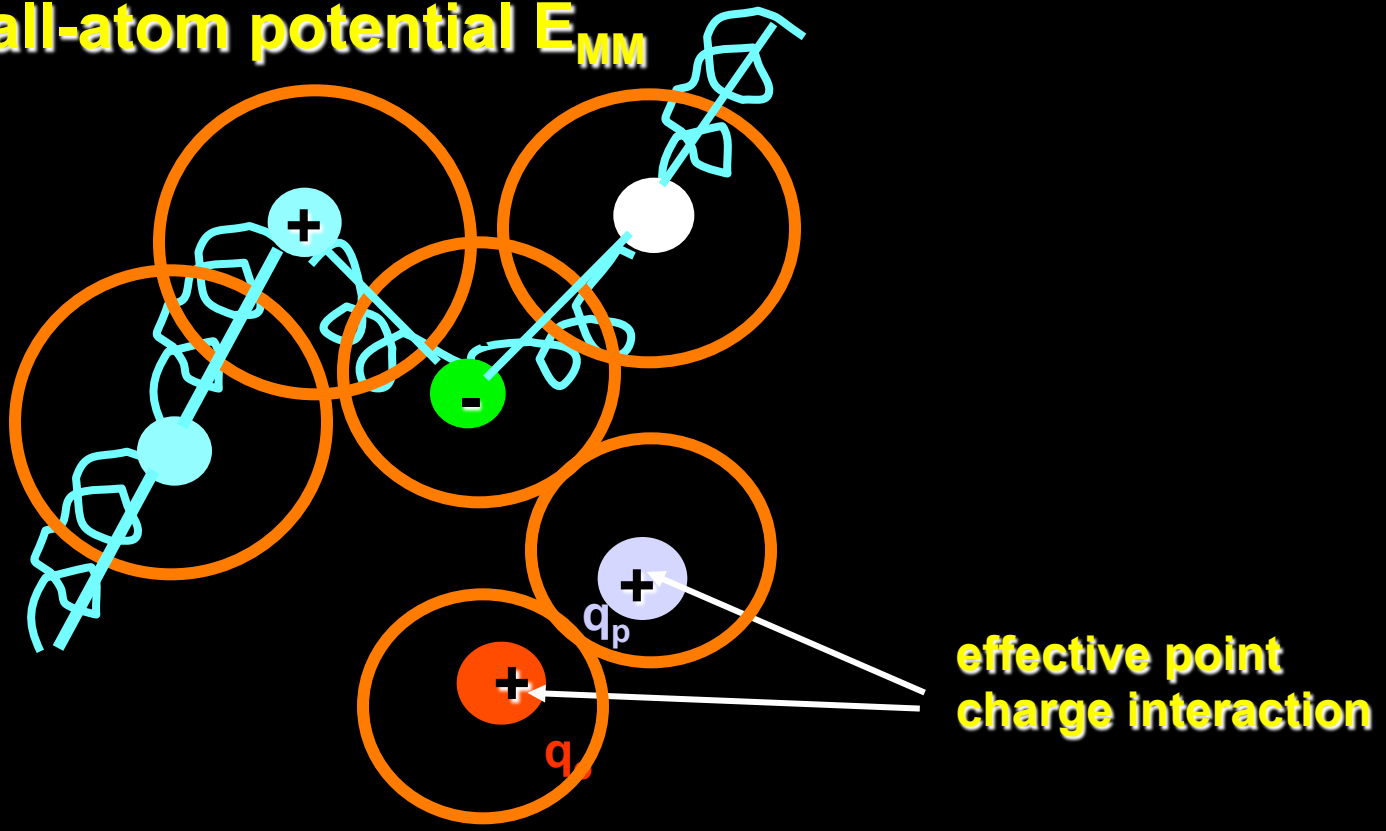

$$E = \sum_b \frac{1}{2} k_b (r_{ij} - b_0)^2 + \sum_\theta \frac{1}{2} k_\theta (\theta_{ijk} - \theta_0)^2 + \sum_\phi \sum_n k_n \left[1 + \cos(n\phi_{ijkh} - \phi_0)\right]$$

$$+ \sum_{lm} \frac{q_l q_m}{4\pi\varepsilon_0 r_{lm}} + \sum_{op} 4\varepsilon \left(\left(\frac{\sigma}{r_{op}} \right)^{12} - \left(\frac{\sigma}{r_{op}} \right)^{6} \right)$$

$E_{QM/MM}$:Bonded Interactions

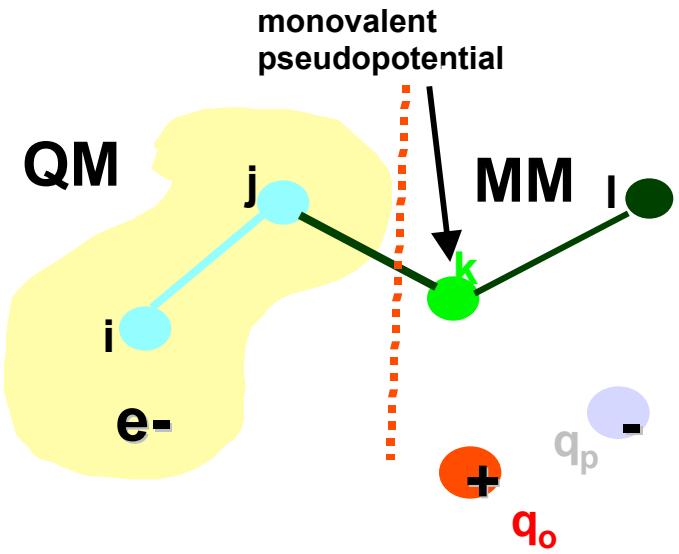

MM atoms/QM atoms bonds: monovalent pseudopotentials

Angle bending and dihedral distorsions:Classical force field

$E_{QM/MM}$:Non bonded Interactions

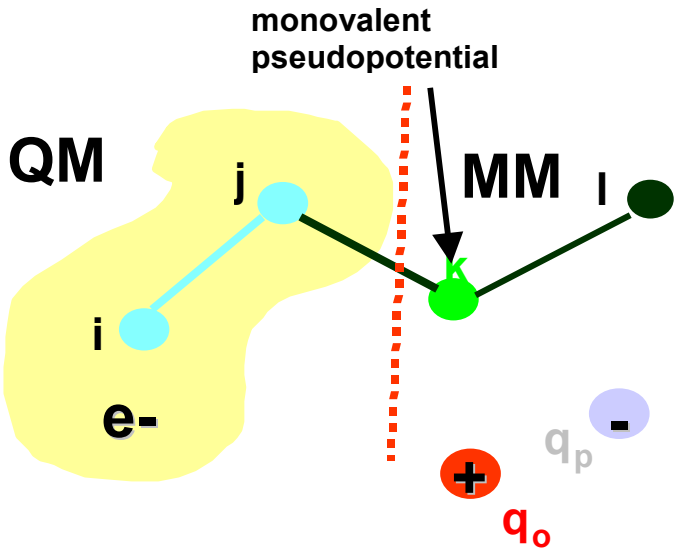

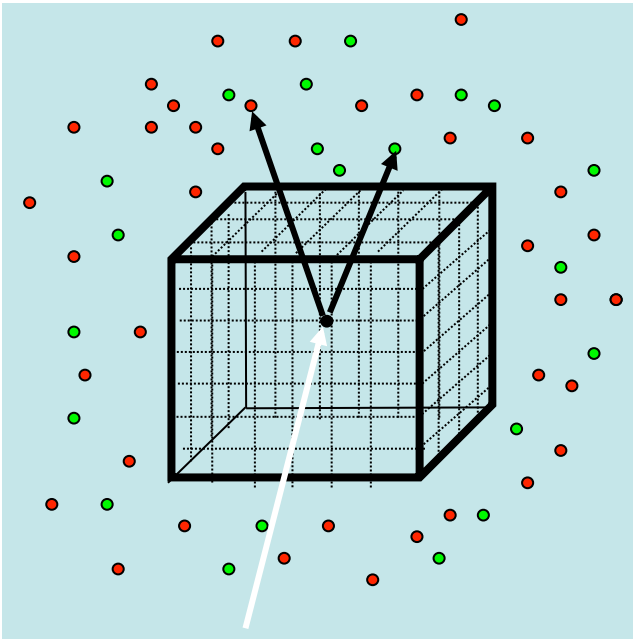

$$E^{st}_{QM/MM} = \sum_{I \in MM} q_I \int dr \rho(r) / |r - R_I| + \sum_{\substack{I \in MM \\ J \in QM}} v_{vdw}(R_{IJ})$$

1-Electron density is overpolarized at short range: *electron spill-out* problem

2- # operations ~N_{rsgrid} x N_{MM} ~1,000 x 10,000

1-Spill out: Replacing the Coulomb potential with an *ad hoc* function

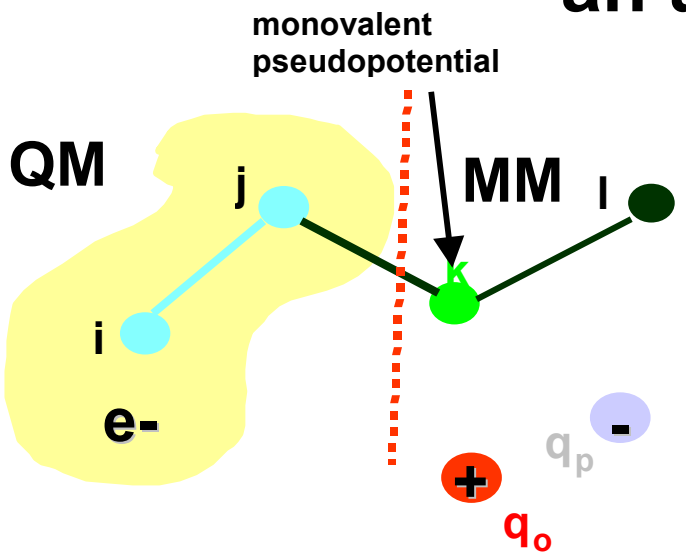

$$E^{ele}_{QM/MM} = \sum_{i \in MM} q_i \int dr \rho(r) v_i(|r - r_i|)$$

$$v_J(r) = \frac{R_{cJ}^4 - r^4}{R_{cJ}^5 - r^5}$$

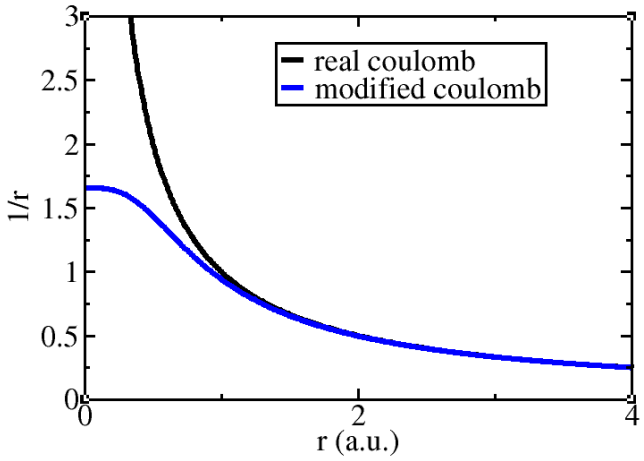

R_{CJ}=cutoff radii, tested in Laio et al JCP 2002

2-Computational Cost: Multiple Scheme

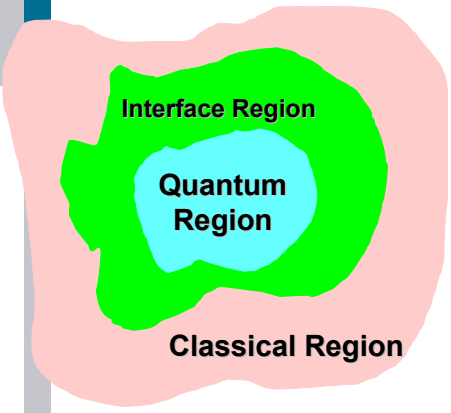

1-Calculate integral only
for a subset of NN atoms
2- For the MM atoms use multiple expansion

CPMD/MM simulations of the K^+ channel

K1=0.91

Wat=0.03

K2=0.87

K3=0.90

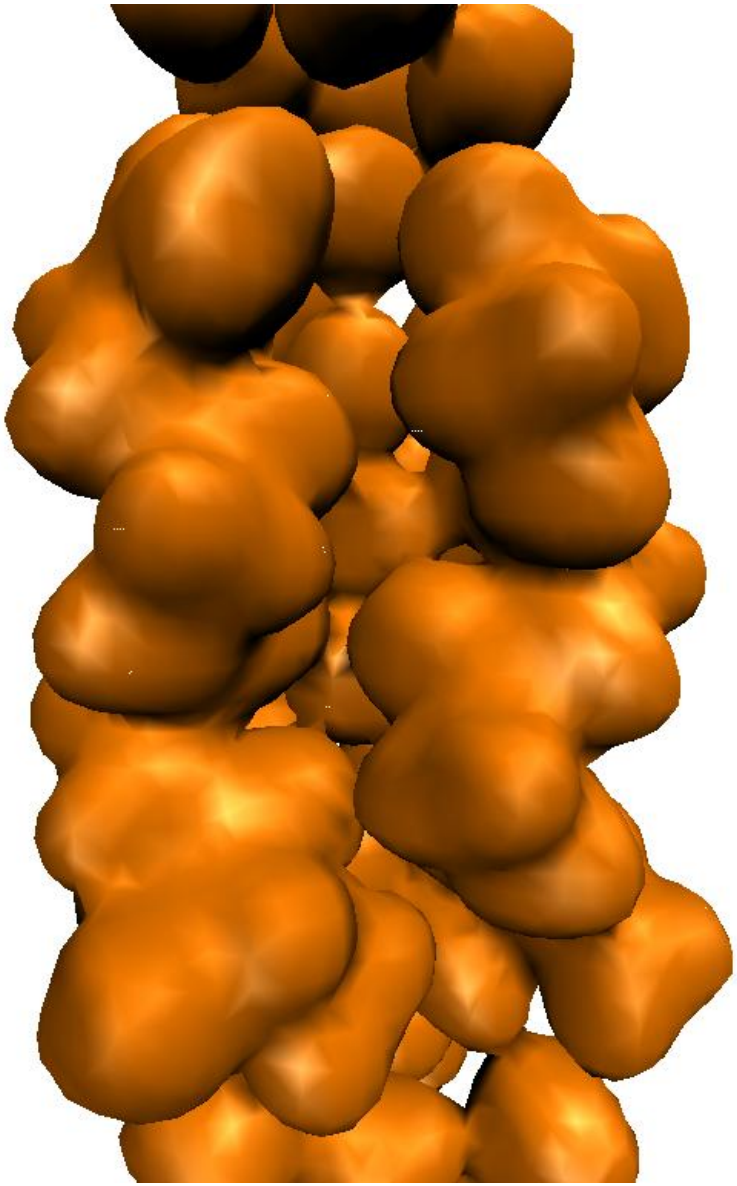

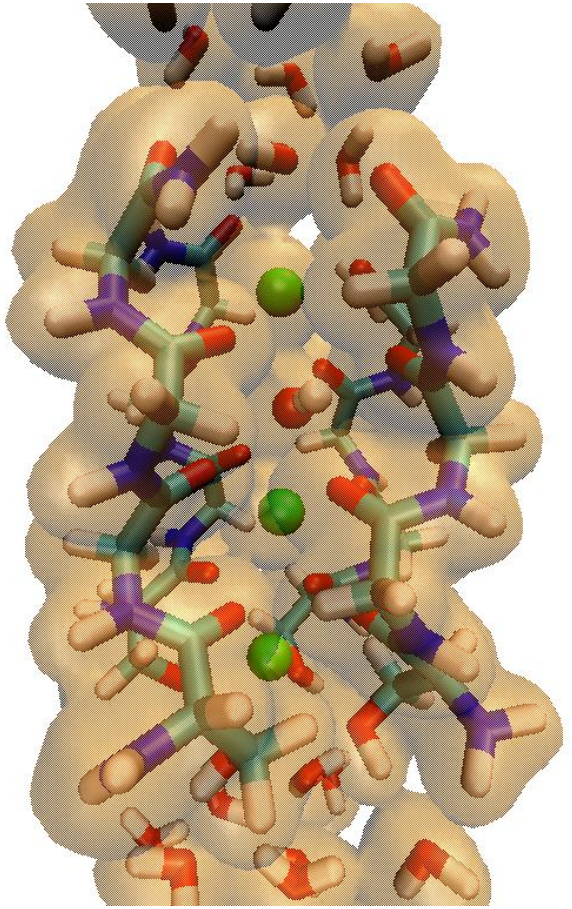

Bucher, Guidoni, PC, Rothlisberger U.
Biophys J. 2010

Protein-Protein interactions in Protein cascades:

The example of olfaction.

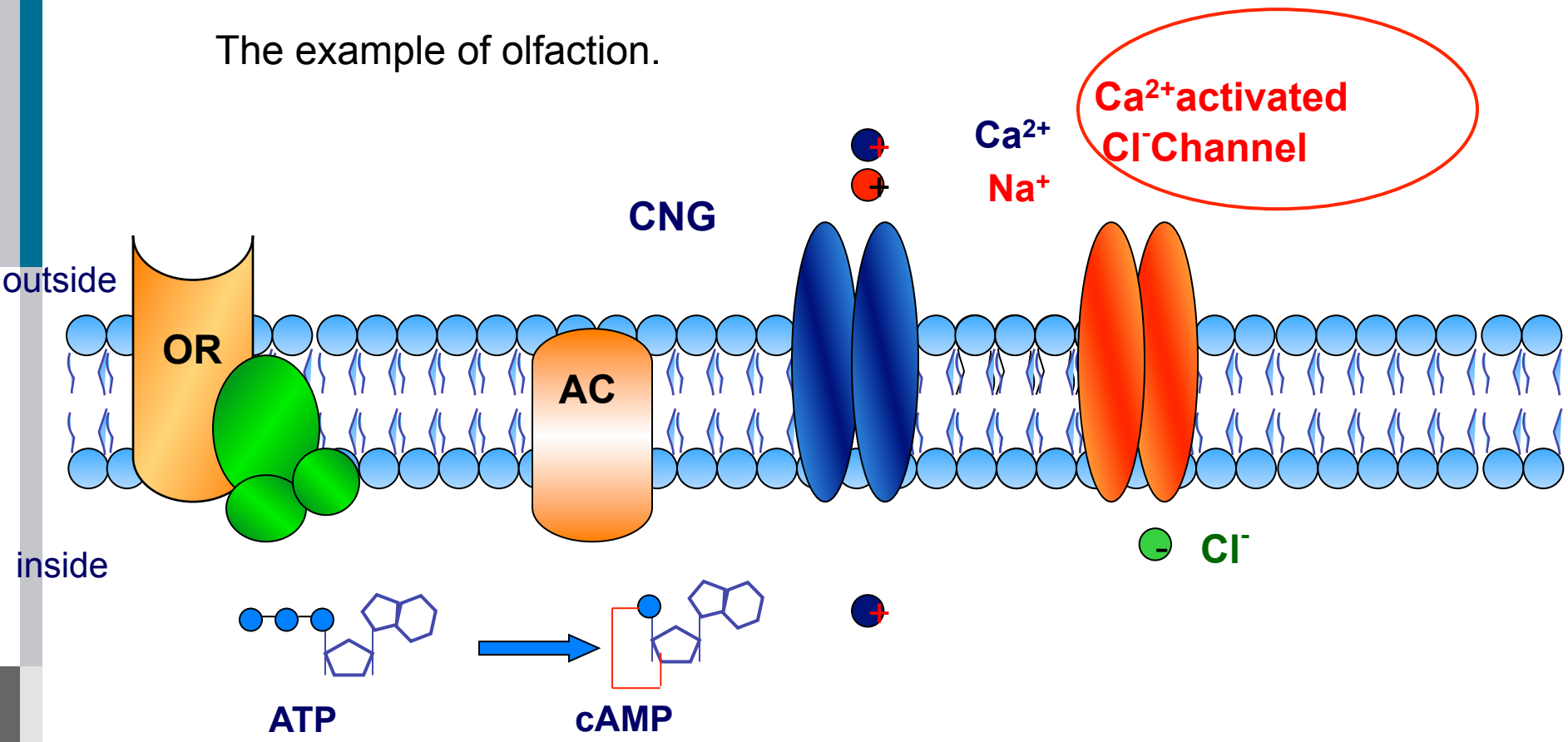

Calcium activates calmodulin protein

Protein-Protein Interactions by all atom MD

JÜLICH FORSCHUNGSZENTRUM

2768 Biophysical Journal Volume 91 October 2006 2768–2777

Using Metadynamics to Understand the Mechanism of Calmodulin/Target Recognition at Atomic Detail

G. Fiorin,* A. Pastore,† P. Carloni,* and M. Parrinello‡

*International School for Advanced Studies and Democritos Modeling Center for Research in Atomistic Simulation, 34014 Trieste, Italy; †Division of Molecular Structure, National Institute for Medical Research, London NW7 1AA, United Kingdom; and ‡Computational Science, Department of Chemistry and Applied Biosciences, ETH Zurich, CH-6900 Lugano, Switzerland

(a)

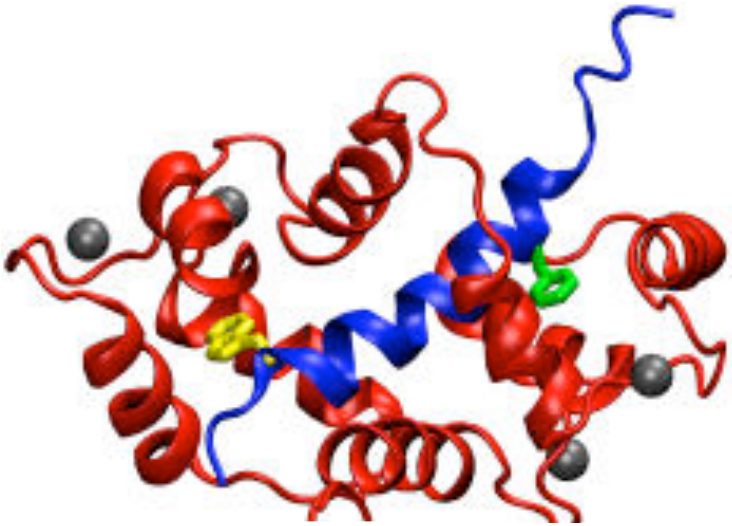

(b)

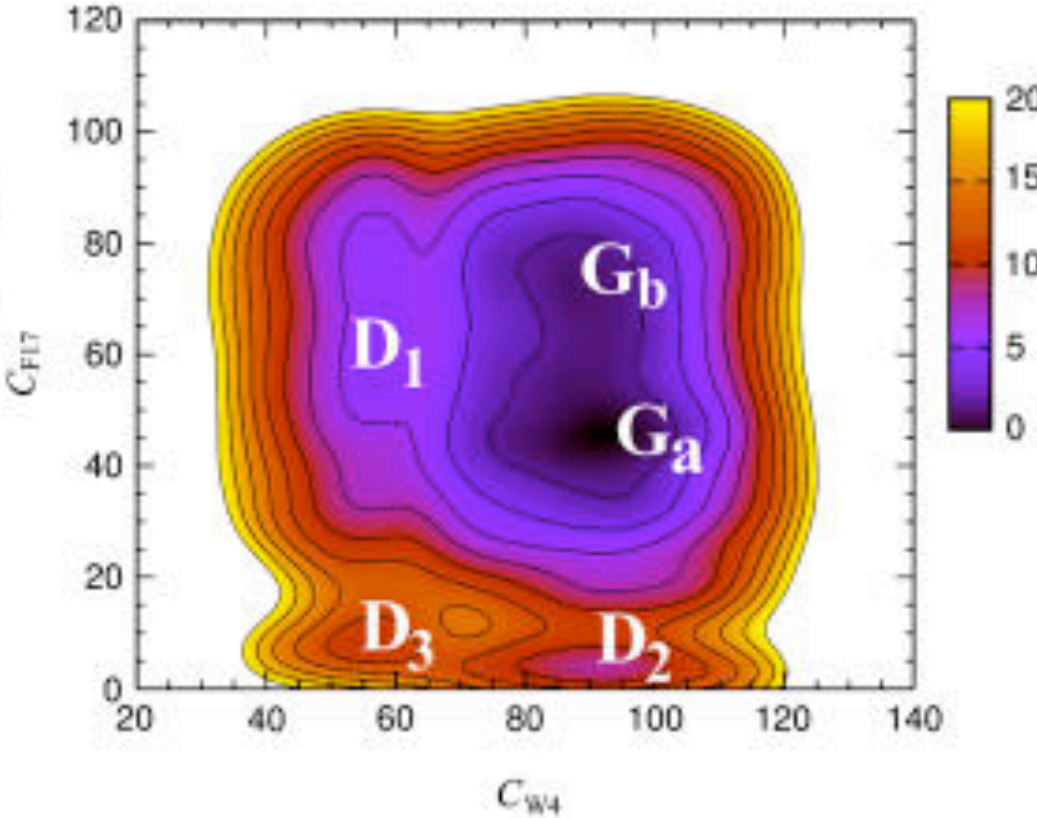

$$\mathcal{L} = -\frac{1}{2}\sum_I M_I \dot{\mathbf{R}}_I^2 \cdot \qquad - E_{MM}$$

Ions and chemicals across And thru membranes

Proton Transfer

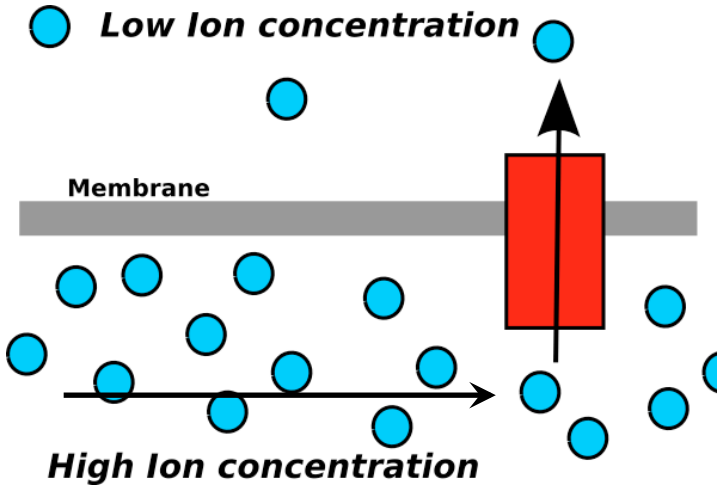

Metal Ion Transfer

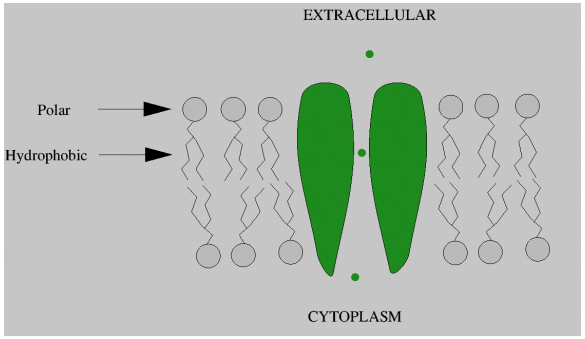

Binding of chemicals

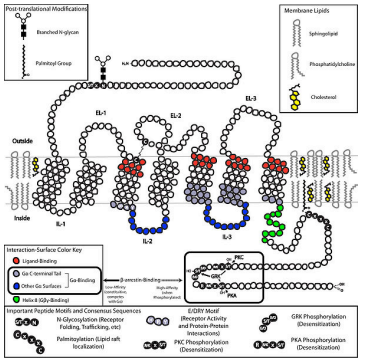

Odorant and Bitter Taste Receptors are GPCR

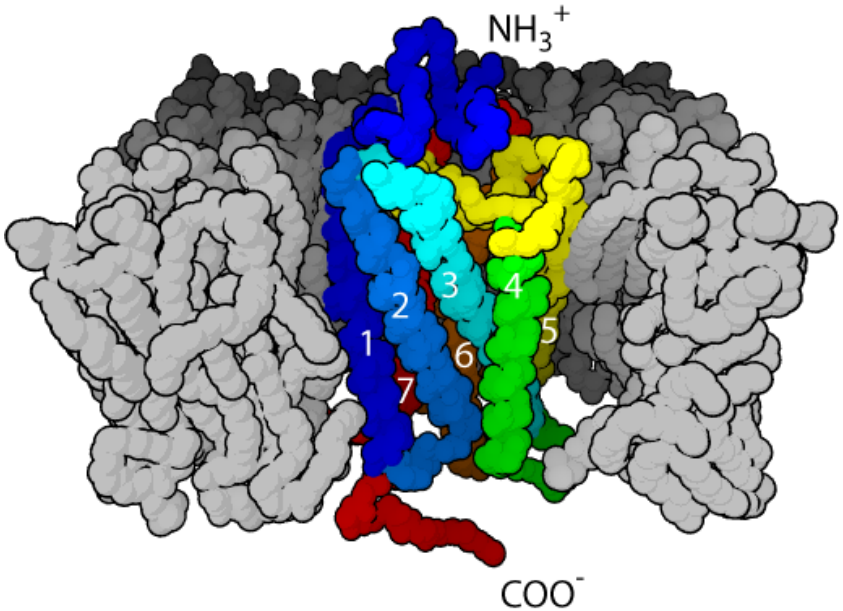

~3%

of mammalian genes

~80%

signal transduction pathway across cell membrane

~30%

of marketed drugs

Nobel Prize in Chemistry 2012 to Robert J. Lefkowitz and Brian K. Kobilka "for studies of GPCR's"

Homology models

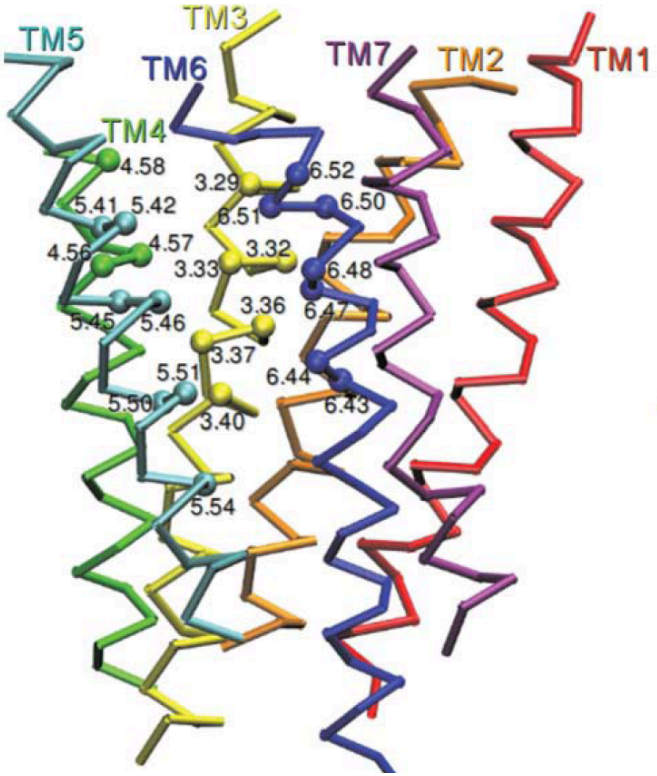

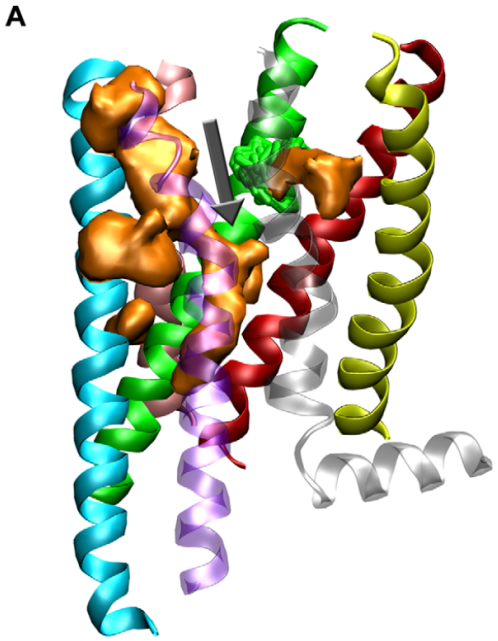

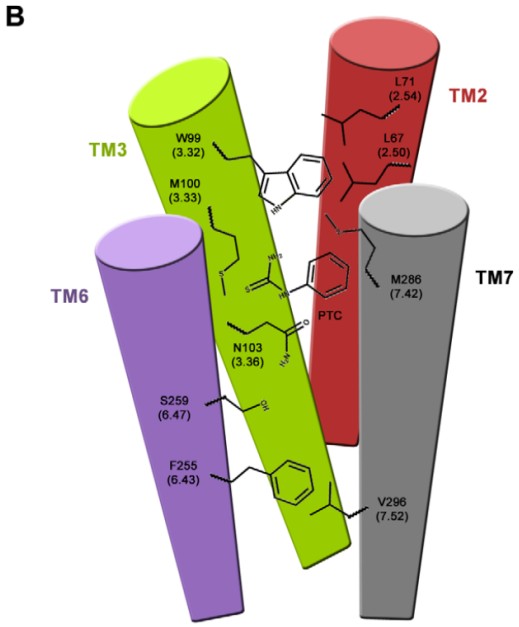

Odorant receptor

Lupieri et al., HFSP Journal , 2009

Bitter taste receptor

Biarnes et al. PlosONE 2010

MM/CG approach

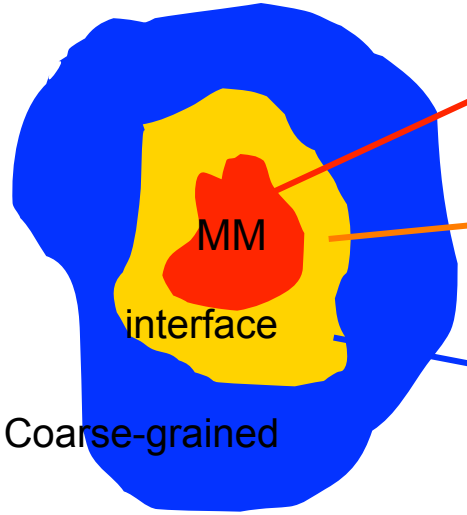

MM region (force field) $\{r_i\}$

Interface region connects the MM and CG (force field)

$\{r_i^I\}$

Coarse-grained region uses the Go-Model residues replaced with Cα

$\{R_i\}$

Test #1: HIV-1 Protease

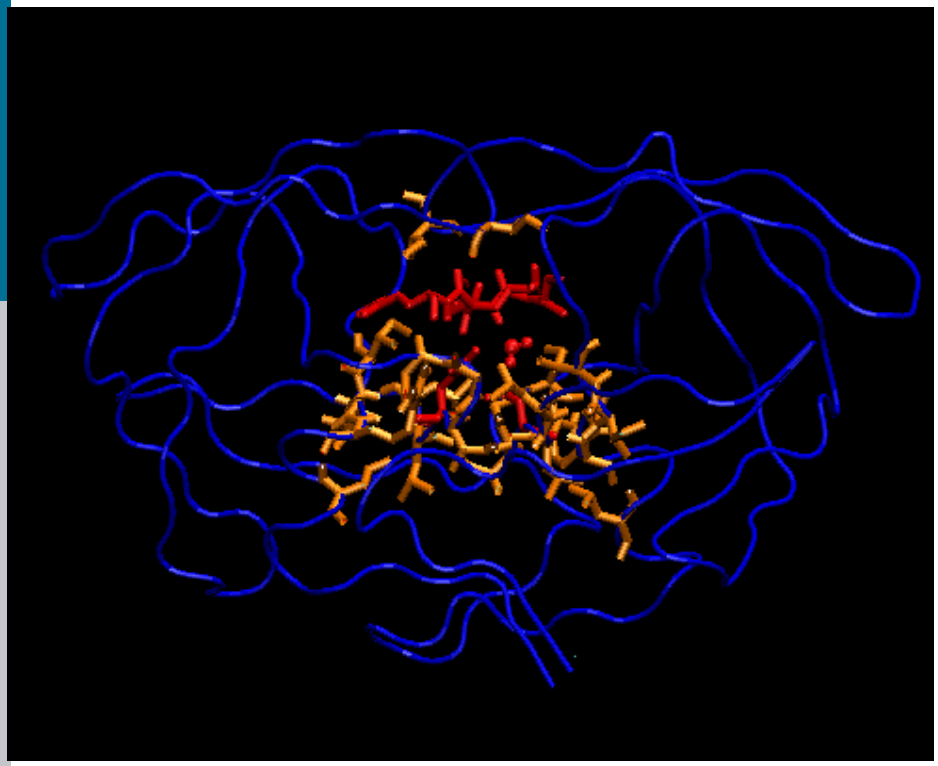

PRL 95, 218102 (2005) PHYSICAL REVIEW LETTERS week ending 18 NOVEMBER 2005

Coarse-Grained Model of Proteins Incorporating Atomistic Detail of the Active Site

Marilisa Neri,[1] Claudio Anselmi,[1] Michele Cascella,[2] Amos Maritan,[3] and Paolo Carloni[1,*]
[1]*SISSA/ISAS and INFM-DEMOCRITOS Modeling Center, Via Beirut 4, I-34014 Trieste, Italy*
[2]*Ecole Polytechnique Fédérale de Lausanne (EPFL), CH-1015 Lausanne, Switzerland*
[3]*Dipartimento di Fisica and INFN, Università degli Studi di Padova, Via Marzolo 8, I-35131 Padova, Italy*
(Received 20 April 2005; published 16 November 2005)

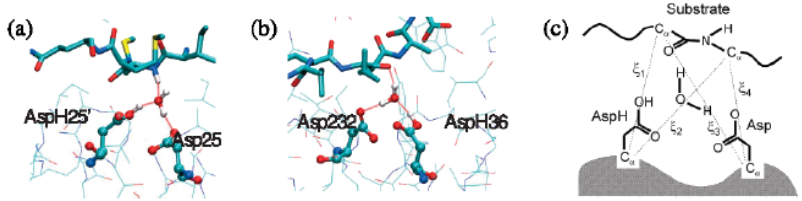

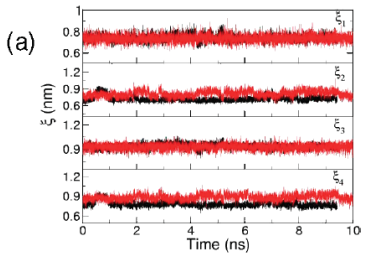

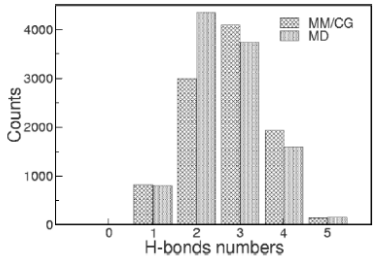

TAS2R38 bitter taste receptor: agonists binding GC/MM simulations

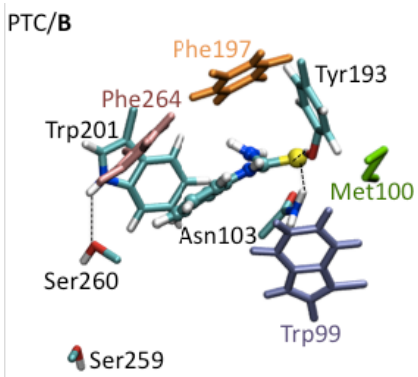

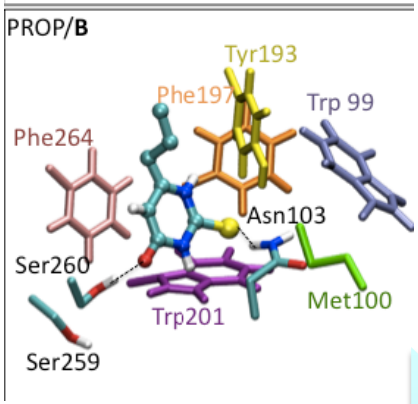

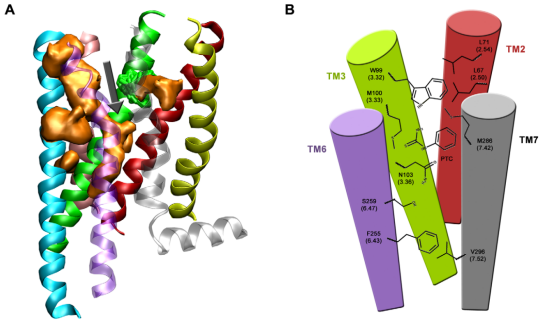

Mutants disrupting agonist/protein interactions

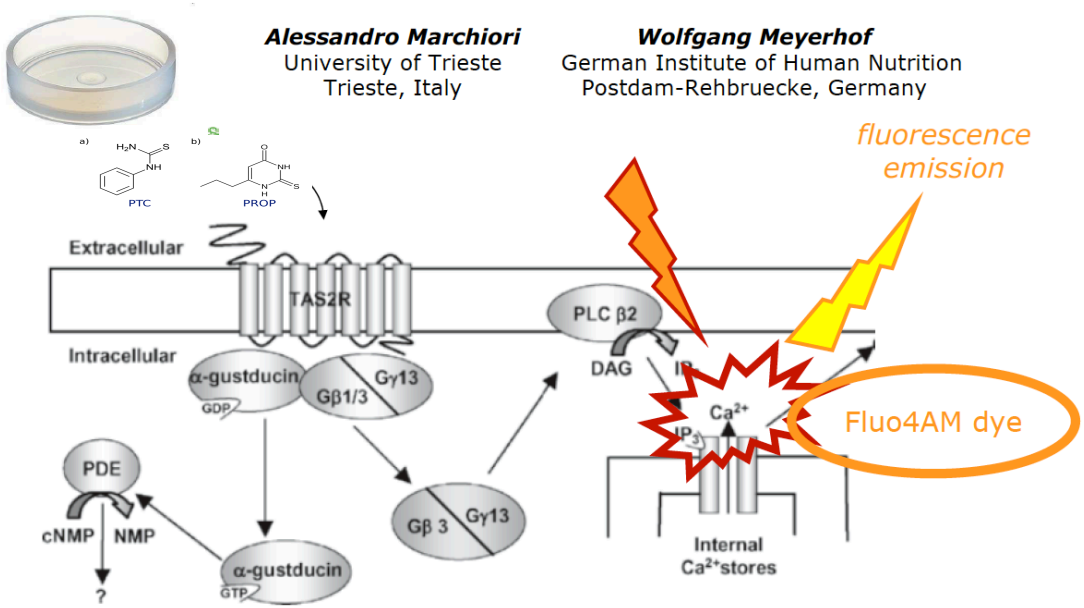

TAS2R38 bitter taste receptor: agonists binding from μs GC/MM simulations

Agonists interact with Asn103, Phe197, Phe264 and Trp201.

They do not interact with the so-called extra cellular loop 2, involved in cis-retinal binding in the GPCR rhodopsin

Predictions are consistent more than 20 site-directed mutagenesis and functional calcium imaging experiments

Variant	Agonist			
	PTC		PROP	
	EC_{50} (uM)	Max act	EC_{50} (uM)	Max act
WT	2.5 (**3**)	0.43 (**0.47**)	2.17	0.44
Trp99 Ala	1.2 (**4.25**)	0.14 (**0.25**)	1.8	0.59
Trp99 Val	1.8 (**2.7**)	0.28 (**1.12**)	5~	0.93
Met100 Ala	4.1 (**3**)	0.72 (**1.01**)	1.2	0.77
Met100 Val	21.2* (**10**)	0.51 (**0.79**)	1.8	0.42
Asn103 Ala	6.6* (**8**)	0.21 (**0.38**)	8.7*	0.65
Asn103 Val	6.9* (**15**)	0.09 (**0.09**)	9.1*	0.41
Asn103 Asp	-	0.06	23.8*	0.13
Asn179 Ala	4.4	0.34	4.9	0.32
Asn179 Val	4.9	0.29	5	0.30
Arg181 Ala	2.2	0.26	4.3	0.26
Arg181 Val	4.5	0.17	7.5	0.19
Asn183 Ala	4.2	0.36	5.3	0.32
Asn183 Val	2.5	0.44	3.1	0.40
Phe197 Val	4.3	0.06	9.9*	0.12
Trp201 Leu	-	0.25	-	0.02
Trp201 Phe	21*	0.14	-	0.05
Ser259 Ala	5.7 (**5.4**)	0.55 (**0.42**)	2.9	0.45
Ser259 Val	99* (**27**)	0.02 (**0.04**)	21.8*	0.18
Ser260 Ala	1.41	0.21	1.14	0.45
Ser260 Val	9.8*	0.03	6.8*	0.09
Phe264 Ala	-	0,06	-	0,06
Phe264 Val	12.4*	0.06	25.9*	0.24

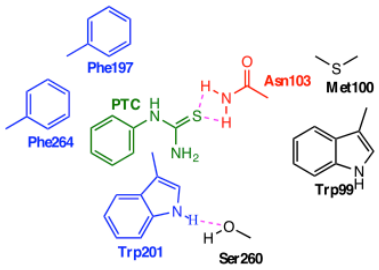

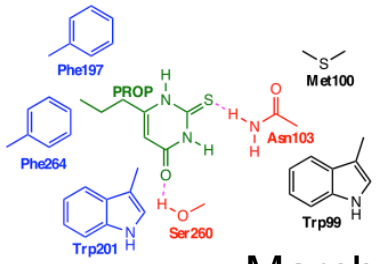

Marchiori et al., PlosONE, 2013

Cell Membrane: Current challenges

JÜLICH FORSCHUNGSZENTRUM

1. Biological environment;real membranes
2. Time-scale and quantum nature of processes at membranes; transition metal ions (e.g. copper transport)
3. Non-equilibrium Thermodynamics
4. Paucity of structural information
5. Action Potential
6. **Cascades**

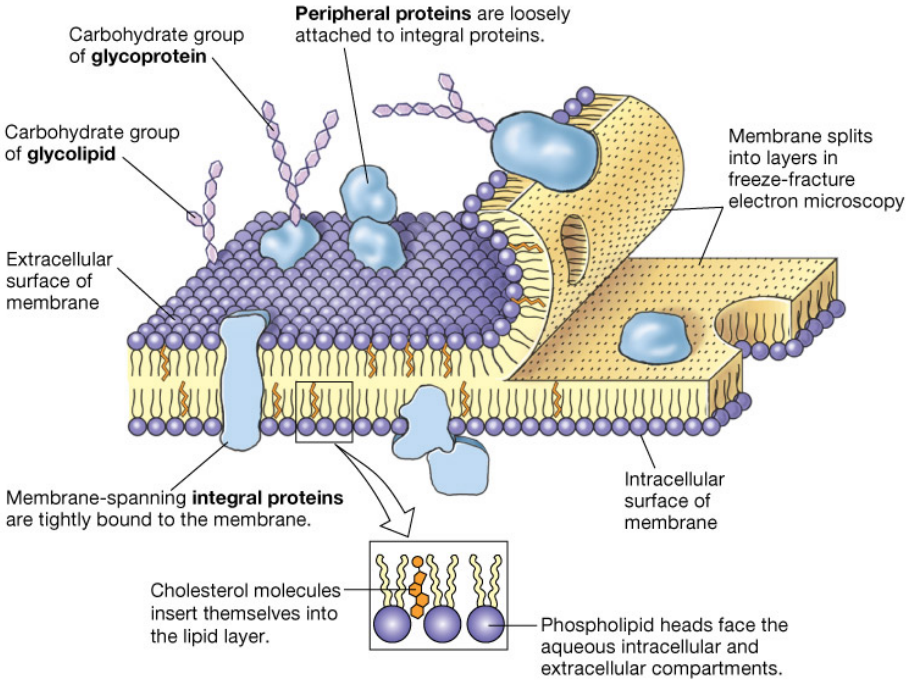

Acknowledgements

Ion Transfer
Peter Pohl (U. Linz, Austria)
Jens Dreyer
Emiliano Ippoliti
Chao Zhang

Chemical Senses
Wolfgang Meyerhof (German Institute of Human Nutrition, Nuthetal, Germany)
Alessandro Marchiori
Luciana Capece
Chuong Nguyen
Alejandro Giorgetti (U. Verona, Italy and GRS)

DFG Deutsche Forschungsgemeinschaft
Bundesministerium für Bildung und Forschung
Ministerium für Innovation, Wissenschaft, Forschung und Technologie des Landes Nordrhein-Westfalen
NRW.
PRACE
illy
DAAD Deutscher Akademischer Austausch Dienst German Academic Exchange Service